

Local Void vs Dark Energy: Confrontation with WMAP and Type Ia Supernovae

Stephon Alexander^{a,*}, Tirthabir Biswas^{a,†}, Alessio Notari^{b,‡} and Deepak Vaid^{a,§}

^a *Department of Physics,
Institute for Gravitation and the Cosmos,
The Pennsylvania State University,
104 Davey Lab, University Park, PA,16802, U.S.A*

^b *Physics Department, McGill University,
3600 University Road, Montréal,
QC, H3A 2T8, Canada and
CERN, Theory Division,
CH-1211 Geneva 23, Switzerland*

(Dated: October 22, 2018)

It is now a known fact that if we happen to be living in the middle of a large underdense region, then we will observe an “apparent acceleration”, even when any form of dark energy is absent. In this paper, we present a “Minimal Void” scenario, i.e. a “void” with minimal underdensity contrast (of about -0.4) and radius ($\sim 200 - 250$ Mpc/h) that can, not only explain the supernovae data, but also be consistent with the 3-yr WMAP data. We also discuss consistency of our model with various other measurements such as Big Bang Nucleosynthesis, Baryon Acoustic Oscillations and local measurements of the Hubble parameter, and also point out possible observable signatures.

PACS numbers:

I. INTRODUCTION

One of the most baffling problems in cosmology and fundamental physics today concerns the acceleration of the universe, as inferred from the redshifting of the type Ia supernovae. Along with this observation, the WMAP data and the large scale structure measurements can all be explained by invoking a dark fluid with negative pressure dubbed as dark energy. This has given rise to the so-called flat Λ CDM or concordance model consisting of approximately only 4% of visible matter (baryons), the rest being dark (approximately 3/4 dark energy and 1/4 dark matter). However, what is this dark energy and why its abundance should be such that it happens to be exactly in concordance with matter density today, remains very much a mystery.

Recently, a few researchers have tried to take a different point of view: what if the effect of large scale structure could account for the observed luminosity to redshift behavior of type Ia supernovae (*i.e.* give rise to an “apparent” acceleration of the universe), without Dark Energy? This question is important because an affirmative answer might obviate the need for a dark energy component/cosmological constant, which has presented a plethora of unresolved theoretical issues. Recent studies of exact solutions to the Einstein equations have, in fact, been able to reproduce the observed luminosity to redshift relation that is usually attributed to acceleration, provided that we lived in a large region (“void”) that has less matter density than the spatial average density over the cosmological Horizon [1, 2, 3] (see [4] for a review). One might naively conclude that this result can obviate the need for dark energy. However, in order for the void model to be taken seriously, several key issues have to be addressed.

Firstly, the observation of small, nearly scale invariant CMB temperature fluctuations, strongly supports the principle that our universe is homogeneous and isotropic on large scales. In our present Universe non-linear large scale structures exist, marking a deviation from homogeneity; however, according to our current understanding of structure formation, $\mathcal{O}(1)$ non-linearities are only expected typically at scales $\sim \mathcal{O}(10\text{Mpc}/h)$. In this case one can again argue that the

*Electronic address: stephon@slac.stanford.edu

†Electronic address: tbiswas@gravity.psu.edu

‡Electronic address: notari@hep.physics.mcgill.ca

§Electronic address: deepak@phys.psu.edu

effect of these inhomogeneities on cosmology, which is governed by the Hubble scale $\sim 3000\text{Mpc}/h$, would be too small to be significant. However, there are reasons why one could be wary of such a conclusion.

From the theoretical point of view, the non-linear behaviour of structure formation is not a trivial issue. For instance, due to non-linear effects it is known that smaller voids can percolate to form much larger underdense structures which occupy most of the volume of the Universe (see *e.g.* [5], according to which such a percolation has a threshold, when the density is about 50% lower than the average), forming what is known as a “cosmic web” of superclusters and voids. Also, we note that non-standard features on the primordial power spectrum, such as a spike at a particular scale, or some non gaussianity may enhance the possibility of having larger structures and voids.

Observationally speaking, several huge nonlinear structures (notably, the Sloan Great Wall has a length of $400/h$ Mpc [6]) have been revealed through surveys like SDSS and 2dF (of course, these data are only tracing the visible matter, so their interpretation in terms of total matter is subject to a bias). It is unclear whether the presence of these large observed objects is consistent with the present understanding of structure formation. For example Einasto [7] claims a discrepancy (by a factor of 5) between the observed abundance of such objects (superclusters) and the values obtained using N-body numerical simulations. Peebles has also argued that our understanding of structure formation and observed voids are in apparent contradiction [8], and that this can be classified as a ‘crisis’ of the Λ CDM model. Further, there has been observational evidence for the presence of a local large underdense ($\sim 25\%$ less dense) region (that extends to $\sim 200\text{Mpc}/h$) from number counts of galaxies [9]. This represents a 4 sigma fluctuation, and would be at odds with Λ CDM. More recently, there has been a claim that the presence of the cold spot in the CMB detected in the WMAP sky [10] is also associated with a similar Big Void in the large scale-structure [11]. Intriguingly, the presence of such Big Voids has also been advocated by [12] in order to explain some features of the low multipole anomalies in the CMB data (in addition to the cold spot). Finally we note that two recent papers [13, 14] claim a significant (95% C.L.) detection of an anisotropy in the local Hubble flow in the *Hubble Key Project* data [14] and in the SN Ia dataset [13]. This would be a completely natural consequence of being inside a large local void [15], since, of course, we are not expected to be exactly at the center and the void is not expected to be exactly spherical.

To summarize, the large scale structure of our universe might be richer than we thought, which can have far reaching consequences for cosmology. However, it is fair to say that the presence of large voids becomes more unlikely (thus requiring probably a non-conventional paradigm of structure formation), as the size of the void and the density contrast that we consider become larger. This emphasizes the need to find the “Minimal Void (MV) Model” *i.e.*, with minimal length scale and underdensity contrast that is required to give a *consistent fit* to the supernovae data (the reader will easily recognize that the larger is the void, in general the better is the fit). This is the first goal of our paper. We find that to obtain an acceptable fit (with goodness-of-fit¹ close to 50%) to the current supernovae data one needs “us” to be located roughly centrally (with 10% precision in the radial position) within an underdense region stretching upto a redshift ~ 0.08 . If one is willing to live with a worse fit (goodness-of-fit $\sim 10\%$) then one can even go down to $z \sim 0.055$. The underdensity that is needed is of about $\delta \sim -0.4$. Now, this is a very large region (corresponding to a radius between $160/h$ Mpc and $250/h$ Mpc). However we believe that finding a viable alternative to the presence of Dark Energy is a task which is important enough to consider such possibilities (and, as noted before, similar structures have been advocated for solving other problems in cosmology, as the low- l anomalies and the cold spot in the CMB).

As an aside we note that we obtain analytical expressions for the luminosity-redshift curve for arbitrary density profiles which are excellent approximations even when the local inhomogeneous patch extends up to $\sim 400\text{Mpc}/h$.

The second important issue that one has to address in the context of the MV model is whether it can reproduce the successes of Λ CDM model for many different observations, most notably the WMAP third year data. In this paper we present an analysis of the MV model subject to the WMAP 3yr data using the COSMOMC package [16] developed to perform a likelihood analysis of theoretical parameters using a Monte Carlo Markov Chain (MCMC) method; we refine the analysis of the type Ia supernovae data and we combine them together. We find that using standard statistical analysis, the MV model accounts for the WMAP and SN Ia data while being consistent also with local measurements of the Hubble parameter.

In what follows, we will find a consistent fit to both the WMAP and SN Ia data, provided the Hubble parameter $H_{\text{out}} \equiv h_{\text{out}}/3000\text{Mpc}^{-1}$ outside the void is very low, $h_{\text{out}} \sim 0.45$. Then the void plays the role of providing a higher value for the local measurements of the Hubble parameter ($H_{\text{in}} \equiv h/3000\text{Mpc}^{-1}$). It is exactly this jump in the

¹ The goodness-of-fit for a fit is the probability that, given a set of physical parameters, the data has a χ^2 smaller or equal than the observed value.

Hubble parameter that gives rise to an apparent acceleration. Additionally, in order to fit the CMB, the primordial spectrum has to deviate from the usual nearly flat spectrum. Specifically we try the fit allowing for running of the spectral index in the observed 7 e-folds of the CMB sky. Our best-fit has a low spectral index with a large running. The overall goodness-of-fit to the WMAP 3 yr data for our best-fit model is around 26% as compared to 41% of the Λ CDM model.

We should clarify that although we quote comparative statistics between MV and Λ CDM model, it is only meant as a guide, our aim here is not to compete with the Λ CDM model. According to the Bayesian statistical likelihood analysis of both the supernovae and the CMB data, our best fit MV model is still disfavored by many standard deviations as compared to the concordant Λ CDM model. Crucially however, such an inference is based on assuming a “flat” prior on the value of the cosmological constant. In other words it relies on the a priori assumption that all the values of the cosmological constant are equally likely. According to the Bayesian theory, such a priori probabilities are to be assigned based on theoretical prejudice. Unfortunately our understanding of the cosmological constant is rather incomplete to say the least. As is well known, theoretical expectations suggest an enormously large value $\sim M_p^4$, and even with supersymmetry it’s “natural” value should have been around $(\text{TeV})^4$, in obvious disagreement with our universe. Accordingly, before the discovery of our accelerated expansion, our theoretical prejudice had been to assume that the cosmological constant must in fact vanish possibly due to some symmetry or other theoretical considerations (for a recent review see for instance [20]). Here we take the same approach, that the “flat prior” assumption may actually be misleading and therefore a direct likelihood comparison between a $\Lambda \neq 0$ model with a $\Lambda = 0$ model may not be appropriate. Rather we should focus on “independent” statistical quantities such as “goodness of fit” which can simply test whether a given theoretical model is consistent with the observational data. In other words, if we had a different theoretical prejudice (for example that a non-zero cosmological constant is “unphysical”), then we could just ask the question whether a non-homogenous matter distribution can fit the data, with an acceptable value of the goodness-of-fit. To summarize, although our model has a worse fit than Λ CDM, in our opinion the statistics suggest that our void model in an EdS background can still be consistent with SN and CMB.

It is natural though to wonder whether one can make these fits better by including perhaps more parameters. We consider two such possibilities in brief. In [17] the authors obtained a slightly better fit to the WMAP data, without Dark Energy, as compared to the Λ CDM model by including a bump in the spectrum at some particular scale (see also [18, 19]). We discuss how this can be integrated in the MV framework. Moreover, this idea looks particularly appealing, because the existence of a bump in the primordial spectrum could, in fact, enhance the probability of finding large voids in the present Universe (the scale of the bump happens to be roughly the scale that we need for a Minimal Void). Next, we consider the possibility of having a slight curvature in the model. It turns out that this also improves the fit to WMAP considerably.

Let us now come to the question of consistency between our model and the measurements of the local Hubble parameter. Although different observations suggest rather different values,

$$0.55 \leq h \leq 0.8, \quad (1)$$

is perhaps a fair range to consider. As we will find out, the supernovae data essentially constrains the amount of jump, h_{out}/h (or equivalently the underdensity contrast in the void), to some range. Combining this with the WMAP analysis (which constrains h_{out}) we get an allowed range for h . These allowed values are definitely low, but we find that our h can be as high as 0.59 and therefore be consistent with the local measurements of the Hubble parameter.

Finally, we briefly discuss consistency of our model with various other measurements, such as baryon acoustic oscillations (BAO), baryon density obtained from Big Bang Nucleosynthesis (BBN), constraints on σ_8 coming from weak lensing experiments, Integrated Sachs-Wolfe (ISW) effect, etc. An important task that we leave for future is to perform an analysis of the SDSS data including Lyman- α forests, without which one cannot really pronounce the MV model as a viable alternative to the concordant Λ CDM model.

We now proceed as follows: in section II, we introduce our swiss-cheese model and briefly discuss the non-linear structure formation captured in this model, as well as the photon propagation in this configuration. In section III we explain qualitatively how the MV model can be consistent with both the supernovae and WMAP data, as well as local measurements of the Hubble parameter. In section IV, we perform supernovae fits for the void model. This includes finding a SN-I best-fit parameter set and comparing it with χ^2 values for the Λ CDM model, as well as finding a combined best-fit parameter set, which has the maximal jump (this will be needed to better fit the WMAP data) with “acceptable” χ^2 . Next in section V, we perform a MCMC analysis of the WMAP data without a cosmological constant. Again, this involves obtaining a WMAP best-fit parameter set, and also finding a Combined best-fit model consistent with supernovae with reasonable χ^2 as compared to the best fit “concordance” Λ CDM model. In section VII, we briefly discuss consistency of MV model with other observations such as BBN and BAO. Finally,

we conclude summarizing our findings and also pointing out unique predictions of the MV model. The appendix contains approximate analytical solution of the trajectory, redshift and luminosity distance of a photon in the radially inhomogeneous “LTB” (Lemaitre-Tolman-Biondi) metric.

II. LARGE SCALE STRUCTURE AND LTB METRICS

As emphasized in the introduction, we are currently living in a universe with significant inhomogeneities: non-linear structures and voids are expected on average at scales $\sim \mathcal{O}(10)$ Mpc/ h , and there is observation of structures up to much larger scales, ~ 300 Mpc/ h . In this paper we will advocate that perhaps we are sitting near the centre of a “Big Void” spanning a radius of ~ 200 Mpc/ h which, as we will explain, is roughly the minimal size needed to account for the SN-Ia supernova data (although one can go down to values of about 150 Mpc/ h by accepting a slightly worse fit).

An accurate way to model such inhomogeneous structures/voids, which avoids any possible pit-falls of perturbative arguments, is to use exact solutions of General Relativity that can be studied both analytically and numerically. In particular we focus on spherically symmetric LTB metrics [21] to describe “radially” inhomogeneous patches of any desired radius, L (such metric describes the most generic spherically symmetric dust-filled spacetime; we refer to appendix IX for definitions and details). Such spherical patches can be pasted onto a homogeneous FLRW metric consistently [22]. It also ensures that the average density inside the spherical patch is the same (almost exactly, see again appendix IX for details) as the background density outside the patch. Thus an underdensity around the central region is compensated by a shell-like structure near the circumference².

Technically, it is somewhat complicated to describe the dynamics of the LTB metric (see appendix IX for details and for the choice we made for the so-called mass function), but intuitively it is as if one had an independent scale factor corresponding to each (comoving) radial coordinate, r , which is evolving as an independent FLRW metric with a given spatial curvature $k(r)$. *A priori*, $k(r)$ is an arbitrary function which also determines the density profile. Assuming $L \ll R_H$ (the Hubble radius) one has

$$\rho(r, t) \simeq \frac{\langle \rho \rangle(t)}{1 + (t/t_0)^{2/3} \epsilon(r)}, \quad \text{where } \langle \rho \rangle(t) \equiv \frac{M_p^2}{6\pi t^2}, \quad \text{and } \epsilon(r) \equiv 3k(r) + rk'(r). \quad (2)$$

We observe that the FLRW behaviour for the density is given by the factor $\langle \rho \rangle(t)$, while the fluctuations are provided by the presence of $\epsilon(r)$ in the denominator. When $\epsilon(r)$ is close to its maximum value we have a void, while when it is close to its minimum, it signals an overdensity. Note that at early times the density contrast $\delta(r, t) \equiv (\rho(r, t) - \langle \rho \rangle(t)) / \langle \rho \rangle(t)$, defined in the usual way, grows as $t^{2/3}$, in agreement with the prediction of cosmological perturbation theory. On the other hand at late times, when $(t/t_0)^{2/3} \epsilon(r) \sim \mathcal{O}(1)$, the density contrast grows rapidly (and this result is the same as found within the Zeldovich approximation [23]). In fact, for an overdense region, the structure ultimately collapses, as to be expected because LTB metrics cannot account for virialization that we observe in nature. Nevertheless, for our purpose, as long as we do not reach the collapse time, LTB metrics adequately capture the effects of non-linear structure formation on photon propagation.

Now, we are interested in modeling a spherical void region surrounded by a compensating shell-like structure, and this is obtained using a $k(r)$ which starts off from a maximum at $r = 0$ and falls off to a constant value at $r = L$ such that

$$k'(0) = k'(L) = 0, \quad (3)$$

$$k(L) = \frac{4\pi}{3} \Omega_k, \quad \text{for } |\Omega_k| \ll 1, \quad (4)$$

One can check that such an LTB metric can consistently match to an FLRW background [22], with curvature abundance Ω_k . In this paper we will mostly focus on a background FLRW metric which is flat. The essential reason for choosing a flat background metric is that curvature is known to be constrained to be very small in order to get a good fit of the WMAP data along with other measurements (such as measurements of the Hubble constant [36]). However, in section ?? we will present a brief discussion on how things may change in the context on the MV model if we allow

² In fact we may speculate that the Great Sloan Wall may be indicative of such a shell-like structure, given its location, at about 250 Mpc/ h away from us, and its two-dimensional shape [6].

for curvature. We note in passing that in LTB models we are considering we do not have back-reaction effects in the outside region, *i.e.* on the average the FLRW regions do not feel at all the presence of holes. The particular choice of the curvature function that we employ to model the inhomogeneities and fit the supernova data is given by

$$k(r) = k_{\max} \left[1 - \left(\frac{r}{L} \right)^4 \right]^2. \quad (5)$$

One can check that Eq.(5) satisfies Eq.(4), in the case with $\Omega_k = 0$. It contains two important physical parameters, L and k_{\max} , which correspond to the length-scale and amplitude of fluctuations respectively³. In the rest of the paper, this is the profile that we will focus on, although some of the analytical results are general for any $k(r)$.

III. THE MINIMAL VOID MODEL

By now in a series of papers [1, 2, 3] it has been shown that a “large” local underdensity can reproduce reasonably well the luminosity distance versus redshift, $D_L(z)$, curve that one observes, and thereby can mimic dark energy (for slightly different approaches based on inhomogeneities, see [24, 25, 26, 27, 28]). However, the reason one is skeptical of such an explanation is because a straightforward extrapolation of the density fluctuations observed in CMB gives us today a scale on nonlinearity (that is, the scale in which the expected density contrast is of $\mathcal{O}(1)$) of at most $\sim \mathcal{O}(10)/h$ Mpc, much too small to explain away dark energy; as we shall see later, we need to invoke a Big Void with a radius of about $200/h$ Mpc (and with average density contrast of roughly $\langle \delta^2 \rangle \simeq 0.4$). The probability of having non-linear structures at larger scales becomes progressively smaller. Using the conventional *linear* and *Gaussian* power spectrum for radii of about ~ 200 Mpc/ h the typical density contrast instead is only of about $0.03 - 0.05$ (for a radius of ~ 160 Mpc/ h the typical contrast is instead about 0.06). However, as argued in the introduction, one cannot take such an analysis at its face value. There are both theoretical and observational suggestions that we might actually have larger underdensities in such voids in our universe.

Nevertheless, it is clear that the presence of large voids becomes more and more unlikely (or that it would require a non-conventional paradigm of structure formation) as the size of the void and the density contrast become larger and larger.

This emphasizes the need to find the “Minimal Void Model” *i.e.*, with minimal length scale and underdensity contrast that is required to give a consistent fit to the supernova data. This is obtained by realizing that the crucial evidence for acceleration comes from the fact that we observe a mismatch between the expansion at low redshifts (between roughly $0.03 \leq z \leq 0.07$) and the expansion at higher redshifts (where supernovae are observed [29], between roughly $0.4 \leq z \leq 1$). This situation arises because of the current experimental status of supernovae observations: we have very few data in the redshift range between 0.07 and 0.4 (the situation will dramatically change with the coming release of the SDSS-II supernovae data [30]). Thus it is not necessary to alter the EdS $D_L(z)$ all the way up to $z \sim \mathcal{O}(1)$, but a large correction to the Hubble expansion in the local region, $0.03 \leq z \leq 0.07$, stretching up to ~ 200 Mpc/ h , may be sufficient. In particular if we are living in a local underdensity, then we experience extra stretching as voids become “more void” (that is how structure formation works) which manifests as a local Hubble expansion rate larger than average (outside the patch), precisely what is required to mimic acceleration. Another way of seeing this is that all sources in the local region have a collective radial peculiar velocity due to the gravitational attraction of the shell-like structure, which adds to the overall expansion.

We may also note that recently [31] has claimed a possible detection of a jump in the supernova Hubble diagram, exactly in the direction of having a large void. However the void radius (about 75 Mpc/ h) and the jump (about 7%) are smaller than what we are proposing.

Let us now see more precisely how the MV model works. Let us start with the observation that the $D_L(z)$ corresponding to Λ CDM model is in good agreement with the observed supernovae [32]. Thus, if we can ensure that our MV model can approximately agree with the Λ CDM $D_L(z)$ curve both in the low and high redshift supernovae range, then we can expect to find a good fit to the data as well. We first focus on the high redshift region, *i.e.* outside the

³ The exponent of r/L has been chosen to be equal to 4, but the reader may note that any exponent $n > 1$ is good, as well. Varying n one varies the width of the shell-like structure. The larger the n , the flatter the void, and narrower the structure. However, we choose to stick only to the case $n = 4$, since it already gives us a sufficiently flat profile for the underdense region which we found to improve the supernova fit, and anyhow the whole analysis and discussion is not very much affected by the precise shape of the shell.

LTB patch. In this region the $D_L(z)$ curve of the MV model basically corresponds to that of the homogeneous EdS curve parameterized by the lower average Hubble parameter⁴, h_{out} . Further, in this range of high redshift supernovae, the EdS curve can run very close to the Λ CDM model, albeit with a different, slightly lower, Hubble parameter, h_{out} as compared to the Hubble parameter h of the Λ CDM curve. For instance, if we compare the EdS distance (D_E) with the Λ CDM distance (D_Λ) [33]:

$$\frac{D_E}{D_\Lambda} \equiv \mathcal{R}(z), \quad (6)$$

it turns out that the ratio \mathcal{R} does not change much in the relevant range of high- z supernovae, $0.4 \leq z \leq 1$:

$$\mathcal{R}(0.4)/\mathcal{R}(1) \simeq 1.12. \quad (7)$$

Moreover, the ratio $\mathcal{R}(z)$ itself is proportional to the ratio h/h_{out} . Thus, by choosing the latter ratio appropriately, the luminosity distance of the average EdS model can be made to approximately coincide with that of the Λ CDM one in the redshift range $0.4 \leq z \leq 1$, and consequently one expects that the EdS/MV model will be consistent with the high redshift supernovae.

Next, let us look at the low redshift region. In this region, the $D_L(z)$ curve is basically linear, the slope being given by the Hubble parameter:

$$H_0^{-1} \equiv \lim_{z \rightarrow 0} \frac{D_L(z)}{z} = \frac{3000 \text{ Mpc}}{h}. \quad (8)$$

Thus in order for the MV model to agree with the best-fit Λ CDM, the Hubble parameter inside the LTb patch should coincide with the measured local Hubble parameter. In other words, if the MV model can account for the jump, \mathcal{J} , between the locally measured Hubble parameter h inside the patch, and the lower average Hubble parameter, h_{out} , outside the patch:

$$\mathcal{J} \equiv \frac{h}{h_{\text{out}}}, \quad (9)$$

then we expect to have a good agreement with the supernovae data.

Thus the challenges are

- to quantitatively verify our above hypothesis of being able to find a good fit to the supernovae with an appropriate “jump”.
- to find whether local inhomogeneities in an LTb model can account for such jumps.

Provided we can make this work, such an analysis will also tell us what a good range for the jump parameter is.

As we will see later, we find a very good fit to the SN data (where we use the dataset [29]), with goodness-of-fit $\sim 50\%$, without Λ in the MV models. Assuming our model, a parameter estimation (with likelihood $e^{-\chi^2/2}$) gives at 95% C.L. the following range for the jump parameter:

$$1.17 \leq \mathcal{J} \leq 1.25. \quad (10)$$

On the other hand the fit to the WMAP data will fix the value of the global h_{out} . As we will see in section V, this is the important quantity for the photons that come from the last scattering surface, and not for example the local h . The challenge for the WMAP analysis is first to see whether one can find at all a good fit to the CMB data, without Dark Energy. It turns out that one can (see section V), but, crucially, a reasonable fit of the WMAP data without Λ requires a relatively low Hubble parameter outside the Void:

$$0.44 \leq h_{\text{out}} \leq 0.47, \quad (11)$$

(at 95% C.L.).

⁴ The discrepancy between the LTb and EdS model goes like a Rees-Sciama effect, $(L/r_H)^3$, which is $\sim \mathcal{O}(10^{-5})$, according to [34]. Such a correction is irrelevant for supernovae, while it could be relevant for CMB. We note, however, that [24, 25] find a larger correction in the luminosity distance. The reason for the discrepancy, however, is still unclear to us.

Now, these two constraints (h_{out} from CMB and the \mathcal{J} from Supernovae) can be combined together. And the third challenge now is whether we get a local value h which is consistent with local measurements of the Hubble parameter. Combining the range Eq.(11) with the constraints from SN Eq.(10), we get a reasonable range of

$$0.51 \leq h \leq 0.59. \quad (12)$$

(see fig. 7) and we have to compare this with the local measurements.

These local values typically vary over a wide range. The Hubble parameter measured using supernovae [35] reads $h = 0.59_{-0.04}^{+0.04}$, the Hubble Key Project [36] measures a value of $h = 0.72_{-0.08}^{+0.08}$ (although in [37] a lower value of $h = 0.62_{-0.05}^{+0.05}$ is given, with an improved treatment of Cepheids). Measurements of clusters using Sunyaev-Zeldovich distances [38] (which is based on data at different redshifts, up to $z \simeq 1$) gives a much lower estimate, $h = 0.54_{-0.03}^{+0.04}$ (in EdS), as does measurement at high redshift ($0.3 < z < 0.7$) using gravitational lensing [39]: $h = 0.48_{-0.03}^{+0.03}$ (for a more comprehensive summary see [18]). In fact, the value of h estimated also seem to decrease as one looks at sources with larger redshifts which would be a prediction for the MV model. However, a detailed study of this issue is well beyond the scope of our paper, but we want to emphasize that the local value of the Hubble parameter has a large window, Eq.(1) being perhaps a fair range to consider.

Clearly there is an overlap between Eq.(12) and Eq.(1), which is now consistent with supernovae, WMAP and local measurements of Hubble.

This can now be used to pinpoint the underdensity contrast required in the void. As we will analytically show in the next section (and verify numerically), the jump parameter in LTB models does not depend on the details of the curvature (density) profile, but only on the amplitude k_{max} , or equivalently the maximal underdensity contrast at the center of the void. We find that a central underdensity between 44% and 58% reproduces the relevant range Eq.(10) of the jump parameter, and it is easy to check that this is also consistent with Eq.(1) and Eq.(11). Notice however that the average underdensity is always somewhat smaller than the central value, see *e.g.* fig. IV B.

At this point one may be concerned about the plausibility of the MV model on two different accounts. Firstly, even if we take the observational evidence of the existence of a large underdense region seriously [9], the underdensity contrast required to be consistent with WMAP and supernovae is quite large. Secondly, the local value of the Hubble parameter is certainly on the lower side. Both of these problems can become milder if one could obtain acceptable fits to WMAP with slightly higher h_{out} . In section V we briefly discuss how it may be possible to evade these problems, but a more detailed investigation of these issues is out of the scope of this paper.

IV. SUPERNOVAE FITS

A. Analytical Results

Our aim in this section is to quantitatively fit the supernova data (we use here the dataset from [29]) using the MV model. In order to have better control, we decided to perform both numerical and analytical analysis. As explained in [34], as long as $L \ll R_H$, one can find excellent approximations to the luminosity distance-redshift relation. This, not only helps us physically understand the effects of corrections coming from inhomogeneities better, but also provides us with a non-trivial check on the numerical calculations. In the appendix we have obtained expressions for $D_L(r)$ and $z(r)$ (which can be used to obtain $D_L(z)$ implicitly) for any general profile. We also provide the reader with a summary of all the equations necessary to reproduce the analytic approximation for $D_L(z)$ in Appendix IX F, in a self-contained form. Inside the LTB patch, the redshift as a function of the radial coordinate looks like

$$z \approx \frac{2r}{3t_0} [1 + 2f(3k(r)/\pi)] . \quad (13)$$

while the angular distance is simply given by

$$D_A = r [1 + f(3k(r)/\pi)] . \quad (14)$$

In deriving these formulas we have used a specific choice of the radial coordinate, given in Eq.(55) of appendix IX F, such that r approximately corresponds to the proper distance today.

The luminosity distance, in General Relativity, is always related to the angular diameter distance [41] D_A via

$$D_L = (1 + z)^2 D_A , \quad (15)$$

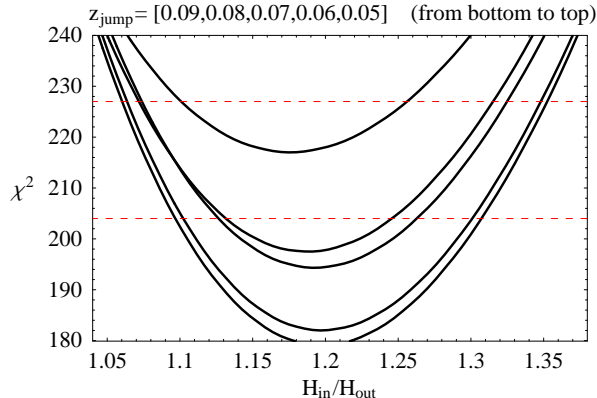


FIG. 1: The χ^2 for Supernovae IA as a function of the jump $h/h_{\text{out}} = H_{\text{in}}/H_{\text{out}}$, for different values of the size of the inhomogeneous region (whose boundary ends at redshift z_{jump}). We have used here a model with two FLRW regions (empty inside and EdS outside), with two different Hubble parameters. From bottom to top the solid curves correspond to $z_{\text{jump}} = [0.09, 0.08, 0.07, 0.06, 0.05]$. The two dashed lines correspond to a 10% and a 1% goodness-of-fit. The number of d.o.f. is 181 (we have used the Riess Gold dataset [29]).

and thus we now have all the ingredients to obtain $D_L(z)$ inside the patch. One can easily verify that, in the above expressions for D_A and z , the terms outside the brackets correspond to the FLRW results for a flat universe. f is an universal function (it does not depend on the profile) defined in the appendix, which gives us the deviation of the $D_L(z)$ curve from the FLRW result. As one can see, our analytical results agree very well with the numerical solutions, see fig.10.

Now, one defines the Hubble parameter as the initial ($z=0$) slope in the $D_L - z$ plot: using this definition one can obtain (see appendix IX D for details) an exact relation between the jump parameter and the central density contrast:

$$\mathcal{J} = \frac{h}{h_{\text{out}}} = 2 - (1 - |\delta_0|)^{1/3}. \quad (16)$$

Surprisingly, this expression does not depend on the specific form of the profile, and therefore lends generality to the analysis.

B. Numerical Analysis

We employ in this section a two steps strategy. First, without even using the LTB metric, we try to fit the data with a crude approximation of the void, which consists of an empty (curvature dominated) FLRW Hubble diagram for the inner region and then an EdS Hubble Diagram for the outer region. Between the two regions ($z < z_{\text{jump}}$ and $z > z_{\text{jump}}$) there is a discontinuous jump in the Hubble parameter $H_{\text{in}}/H_{\text{out}}$. In this way we get a good idea about what are the best values for \mathcal{J} and z_{jump} . The results are shown in fig. 1.

As one can see from the plot, the larger is the value for z_{jump} the better is the fit. However, we do not gain much by taking z_{jump} larger than, say, 0.08 (which corresponds to a radius of 250 Mpc/h). It is also interesting to note that a z_{jump} as low as 0.05 (which corresponds to a radius of 150 Mpc/h) still gives a reasonable fit (goodness-of-fit is higher than a few %). Almost independent of z_{jump} , the best value for the jump is around $\mathcal{J} \simeq 1.2$.

As a second step, then, we try to reproduce these results with a full LTB study. For simplicity we focus on only one value of L for the LTB patch ($z_{\text{jump}} \approx 0.085$). A further observational motivation for considering such a redshift comes from the fact that it also approximately coincides with the redshift of the Sloan Great Wall, which spans hundreds of Mpc across and it could be suggestive of being the “compensating structure” expected at the boundary of the LTB patch [6]. In the profile Eq.(5), we therefore fix the radius L , and let k_{max} vary (which corresponds to varying the jump \mathcal{J} , or equivalently the central density contrast δ_0).

We solve numerically for the $D_L - z$ curve for several values of k_{max} (which correspond to several values of \mathcal{J}), and we compute the χ^2 . We show in fig. (2) the χ^2 as a function of the jump, interpolating between the results of the numerics. This interpolating function is then used to compute the statistics: We find that the 1σ range of the jump

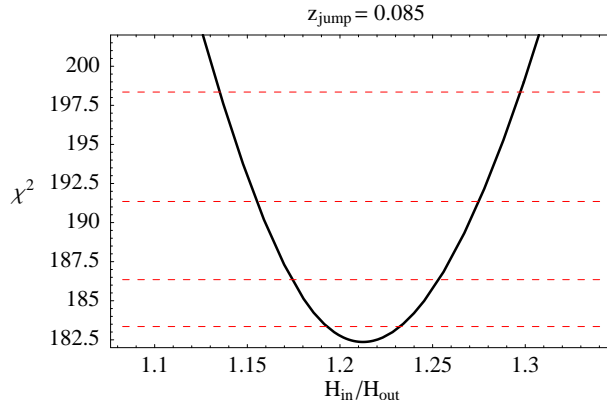


FIG. 2: The χ^2 for Supernovae IA as a function of the jump $h/h_{out} = H_{in}/H_{out}$, in a full specific LTB model, matched to FLRW at redshift $z_{jump} = 0.085$. The dashed lines correspond to the 1σ , 2σ , 3σ and 4σ where we used as a likelihood $e^{-\chi^2/2}$. The number of d.o.f. is 181 (we have used the Riess Gold dataset [29]).

corresponds to $1.214_{-0.019}^{+0.019}$. For the density contrast at the center this translates to $\delta_0 = 0.514_{-0.036}^{+0.034}$.

Let us comment briefly on the values that we get for the χ^2 as compared to other models. The EdS model has a very bad fit to the data, since its χ^2 for the same dataset is about 284. This has a very low goodness of fit. On the other hand the Λ CDM model has a much lower χ^2 than our model ([29] quotes 150)⁵, which is indeed strangely too low⁶. Now, in terms of goodness-of-fit our χ^2 is what one expects typically, since it is roughly equal to the number of d.o.f., and this makes our model a good fit to the data. On the other hand if one allows a new free parameter (Ω_Λ) then the best fit turns out to be at a nonzero value for Ω_Λ , and so the parameter value $\Lambda = 0$ would be formally excluded at several σ (assuming a likelihood that goes as $e^{-\chi^2/2}$). This situation is similar to what we will encounter when we perform the CMB fits (see section V): the MV model has a worse χ^2 as compared to Λ CDM, but the question that we want to ask is about consistency of SN data with a MV model, and for this question the answer seems to be yes, the $\chi^2/\text{d.o.f.}$ being roughly equal to 1.

We also note that we use only one dataset [29] (while there are other ones in the literature), since we would qualitatively get very similar answer and it is not our purpose here to compare dataset with others, but just to check the consistency of the model.

Finally we show, as an illustration, one example of a plot of $D_L - z$ in figure IV B together with the shape of the density profile (as a function of z).

V. MCMC FIT OF THE WMAP DATA

In order for the MV model to be viable at all, it is crucial for this picture to be in agreement with observations of the CMB spectra, among other things. It is commonly assumed that the Λ CDM model, with a non-zero cosmological constant, is the only one which can adequately explain the CMB spectrum. This is based on the result that once one assumes a “flat” prior on Λ , it turns out that the “most likely” parameters, given the WMAP data, correspond to $\Omega_\Lambda \sim 0.7$. The question that we want to ask however, is about consistency of WMAP with EdS: can we get a reasonable fit to the CMB spectrum even after setting Λ to zero? To put it differently, if we had a strong theoretical prejudice against having a non-zero cosmological constant, or if there were other observations disfavoring it, then would the 3-yr WMAP data independently rule out an $\Omega_M = 1$, EdS universe? (Here M means total matter =

⁵ The open empty Universe has also a low χ^2 , of about 160.

⁶ We note here that all the SN fits are plagued by not knowing exactly what are the errors on the SN measurements. In fact, if one used only instrumental errors, then the data points would have a very large scatter with tiny errors, and there is no smooth curve which can give a fit to the data. Then what is done by SN collaborations is to artificially add by hand an error bar of about 0.15 magnitudes in quadrature to all data points, which is typically justified saying that this is the typical variability of the intrinsic SN luminosity. This is what makes the concordance Λ CDM χ^2 so low.

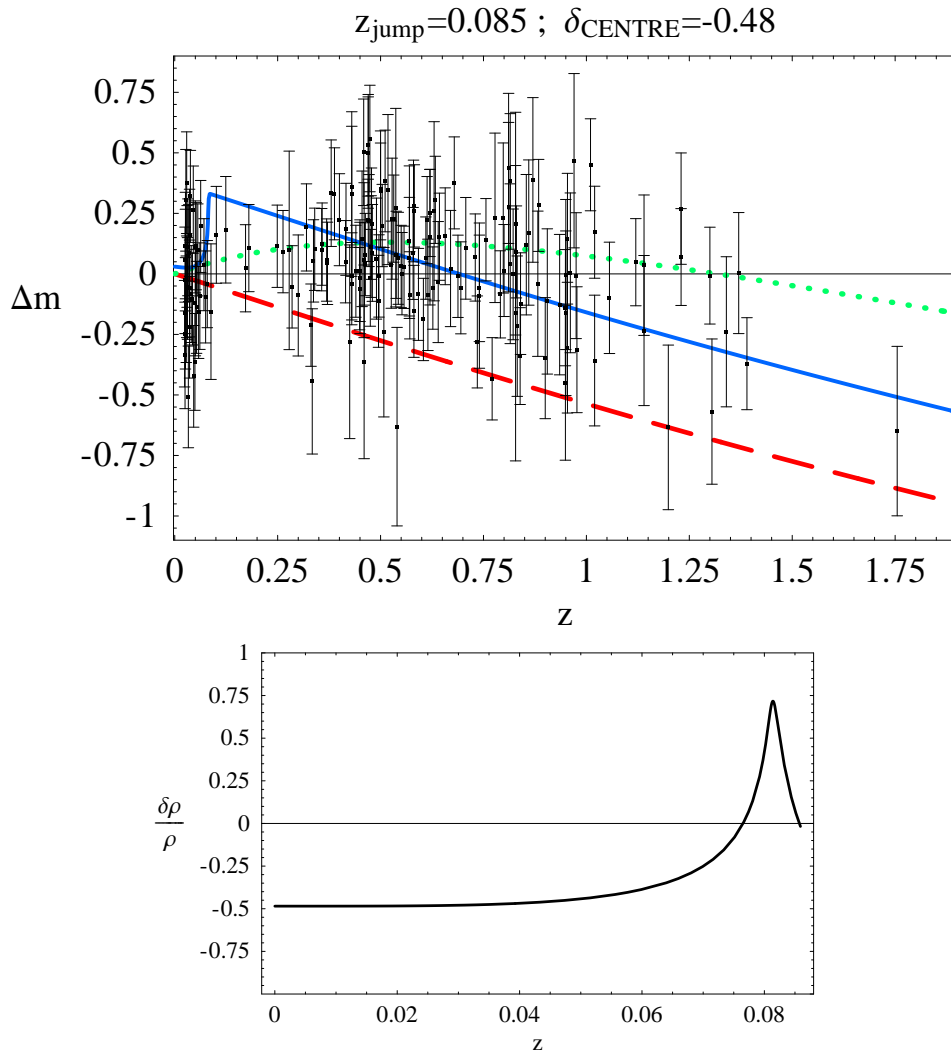


FIG. 3: In the upper plot we show a fit of the Supernovae data (Riess et al. [29]) with an LTB model which has $\chi^2 = 186$ (the d.o.f. are 181). The inhomogeneous patch extends up to $z \simeq 0.085$ and the underdensity in the center is $\delta_{\text{CENTRE}} = -0.48$. We have shown $\Delta m \equiv m - m_{\text{empty}}$: the magnitude ($m \equiv 5 \text{Log}_{10} D_L$) minus the magnitude of an empty open FLRW Universe as a function of the redshift z . The blue solid line is our inhomogeneous model, the red dashed-line is an EdS model (whose Hubble constant is normalized through the nearby supernovae), the green dotted line is the best-fit ΛCDM . In the lower plot we show the density contrast for the same model, as a function of z . The average contrast ($\sqrt{\langle\delta^2\rangle}$) in the inhomogeneous patch is 0.43 ($\sqrt{\langle\delta^2\rangle} \simeq 0.33$ in the underdensity, $\sqrt{\langle\delta^2\rangle} \simeq 0.48$ in the overdensity).

baryons + dark matter.) In particular, what if we introduce additional features in the primordial spectrum, rather than tampering with the composition of the universe? If we indeed obtain a reasonable fit using such a different “prior”, the next important step would be to check whether this parameter set is consistent with the supernovae fit. This is what we plan to do in this section.

Rigorously speaking, this question seems technically challenging because one would have to compute the secondary effects, *i.e.* what the spectrum of the CMB radiation would look like after passing through the local underdense region, and maybe many other such regions⁷, it encounters on its journey to us. According to [34], the corrections to the redshifts of photons which pass through a void of size L is a Rees-Sciama effect that goes like $(L/R_H)^3$. A

⁷ The assumption that we live in a void could naturally lead us to consider that the universe might contain many such voids, a bubbly universe. In this case one would have to compute the passage of the photons through many such voids.

	Λ CDM		EdS $\alpha_s = 0$		EdS $\alpha_s \neq 0$		Curved $\alpha_s, \Omega_k \neq 0$	
	<i>min</i>	<i>max</i>	<i>min</i>	<i>max</i>	<i>min</i>	<i>max</i>	<i>min</i>	<i>max</i>
$\Omega_b h_{\text{out}}^2$	0.005	0.04	0.005	0.04	0.005	0.04	0.005	0.04
$\Omega_m h_{\text{out}}^2$	0.01	0.3	0.01	0.3	0.01	0.3	0.01	0.3
Ω_Λ	0	1	0	0	0	0	0	0
n_s	0.5	1.5	0.5	1.5	0.5	1.5	0.5	1.5
α_s	0	0	0	0	-0.3	0.3	-0.3	0.3
Ω_k	0	0	0	0	0	0	0.05	0.05
z_{re}	4	20	4	20	4	20	4	20
$10^{10} A_s$	10	100	10	100	10	100	10	100

TABLE I: Priors for different parameters in the COSMOMC Runs. Here $\Omega_b h_{\text{out}}^2$ is the physical baryon density, $\Omega_m h_{\text{out}}^2$ is the physical dark matter density, z_{re} is the redshift at re-ionization, n_s is the spectral index, α_s is the running of the spectral index and A_s is the amplitude of scalar fluctuations (for definitions see, *e.g.* [16]).

coherent addition of this effect due to many voids could produce a correction of order $(L/R_H)^2$. Thus for a void with a typical radius $\sim 200/h$ Mpc that we considered in this paper, such a cumulative effect could be $\sim 10^{-2} - 10^{-3}$. This can be ignored for the study of supernovae⁸. On the other hand, if these many voids exist, they would give a sizable effect on the CMB. The number $\sim 10^{-2} - 10^{-3}$ would refer to a monopole in the CMB, while the correction to higher multipoles would be smaller (depending on how different is the number of voids along different directions in the sky). However, in this paper we ignore such secondary effects. On the qualitative side, in fact, we expect this to be important only for small l and decay fast for larger l , and it should act in the same way as an Integrated Sachs-Wolfe effect⁹.

The correction to the CMB redshift that comes from our local void, instead, will depend on how symmetric the void is, and how “centrally” we are located. For an off-center observer, in appendix IX E we perform a non-perturbative estimate of the dipole moment, and find that in order for it to not exceed the observed value $\sim \mathcal{O}(10^{-3})$, “we” must be located very close to the center, approximately within 10% of the void-radius, in concordance with the findings in [42]. In this case the correction to the higher multipoles are much more suppressed and not visible in CMB [42]. Departure from spherical symmetry, on the other hand, may have a much more interesting effect, specially on the lowest l s in the CMB spectrum, and could be visible¹⁰. However, such a study is clearly out of the scope of the present paper; instead we will restrict ourselves to spherically symmetric voids and neglect these possible secondary effects on the CMB coming from the voids embedded in the homogeneous EdS background. Thus, the question reduces to whether the CMB spectrum can be reproduced given an EdS background.

As one would expect, we find that if one assumes as priors, no dark energy, as well as no additional features in the primordial spectrum (other than spectral index and amplitude), one obtains a very poor fit to the 3-yr WMAP data (see table IV). However the situation changes if we introduce a possible “running in the spectral tilt”, α_s , in the observable ~ 7 e-folds of our universe in CMB (following the same definition as in [16])¹¹

We have performed a Monte Carlo Markov Chain (MCMC) analysis of the WMAP 3 year data using the program COSMOMC [16]. Our runs were performed with the priors given in table V. We used the version of the COSMOMC program which lets one analyze the range $2 \leq l \leq 30$ for TT correlations and the range $2 \leq l \leq 23$ for TE+EE correlations using the pixel-based approach (T, Q and U maps), which offers a much more accurate treatment of the low- l likelihood [43]. One has (957+1172) pixel data in all. The rest of the correlations that we considered consisted of C_l^{TT} in the range $31 \leq l \leq 1000$, and C_l^{TE} in the range $24 \leq l \leq 450$.

We find that an EdS universe with *no dark energy* but with a value of the Hubble constant, H_{out} , significantly lower than the conventionally accepted value of ~ 70 km/s/Mpc gives a very reasonable fit to the CMB spectrum, see fig. 4.

⁸ We mention, again, that [24, 25] find a larger correction to the luminosity distance, which could be potentially important for supernovae [24]. Since the reason of the discrepancy is still unclear to us, we do not discuss it here.

⁹ This might explain the claimed detections of ISW correlations [40], even without invoking Dark Energy.

¹⁰ In this context we note that similar effects in anisotropic geometric void configurations have been used to explain the low multipole anomalies in the CMB sky [12].

¹¹ Ideally, one would like to introduce two additional scales where significant running of the spectral tilt starts and ends. This would also obviously improve the fit. However, to keep the analysis simple, we have assumed that these two scales lie outside the observed spectrum in WMAP.

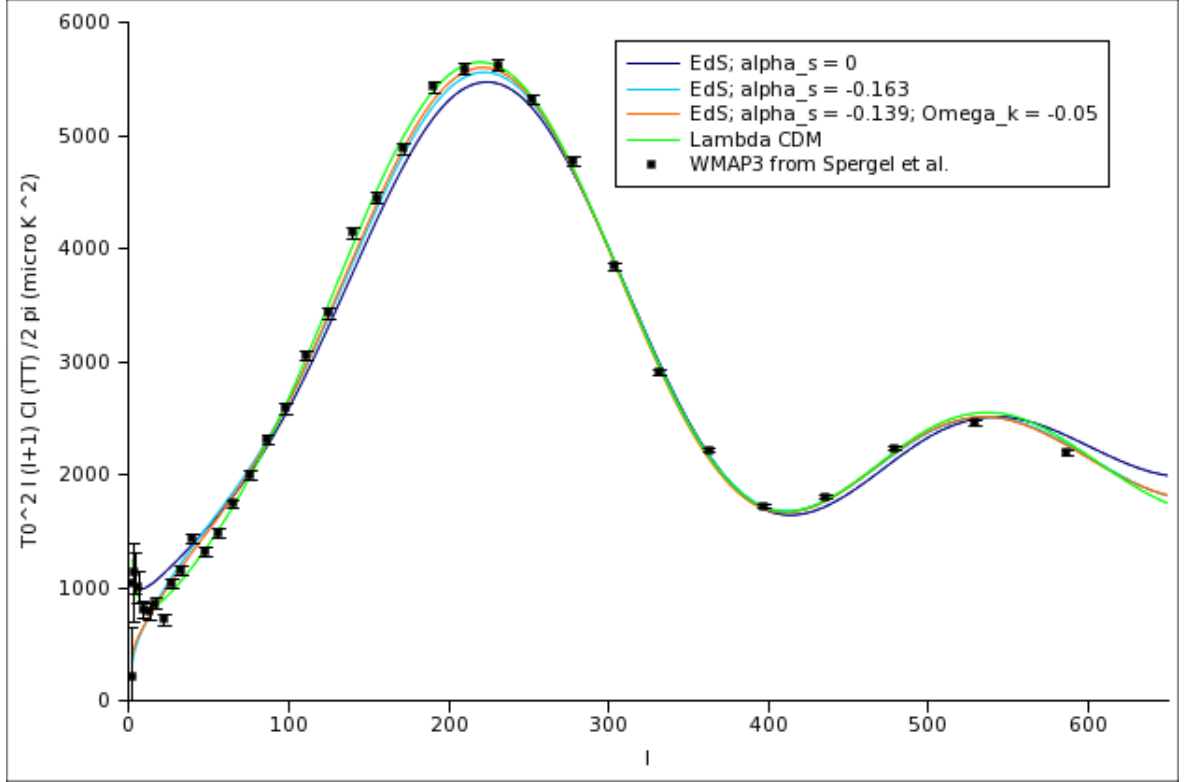


FIG. 4: Λ CDM and EdS fits to the WMAP 3 binned data

	Λ CDM	EdS, $\alpha_s = 0$	Eds, $\alpha_s \neq 0$	Eds, $\alpha_s, \Omega_k \neq 0$
$\Omega_b h_{out}^2$	$0.022^{+0.002}_{-0.002}$	$0.022^{+0.001}_{-0.001}$	$0.018^{+0.001}_{-0.002}$	$0.019^{+0.002}_{-0.001}$
$\Omega_m h_{out}^2$	$0.106^{+0.021}_{-0.013}$	$0.198^{+0.008}_{-0.011}$	$0.186^{+0.011}_{-0.009}$	$0.167^{+0.009}_{-0.007}$
Ω_Λ	$0.759^{+0.041}_{-0.103}$	0	0	0
z_{re}	$11.734^{+4.993}_{-7.619}$	$8.697^{+4.351}_{-6.694}$	$13.754^{+2.246}_{-5.752}$	$13.342^{+2.55}_{-5.011}$
Ω_k	0	0	0	0.05
n_s	$0.96^{+0.04}_{-0.04}$	$0.94^{+0.021}_{-0.038}$	$0.732^{+0.07}_{-0.071}$	$0.761^{+0.069}_{-0.069}$
α_s	0	0	$-0.161^{+0.044}_{-0.044}$	$-0.13^{+0.037}_{-0.048}$
$10^{10} A_s$	$20.841^{+3.116}_{-3.442}$	$25.459^{+2.135}_{-2.766}$	$25.302^{+2.182}_{-2.968}$	$23.975^{+2.198}_{-2.448}$
Ω_m / Ω_b	$4.73^{+0.999}_{-0.485}$	$9.119^{+0.341}_{-0.357}$	$10.094^{+0.645}_{-0.489}$	$8.929^{+0.512}_{-0.541}$
h_{out}	$.72857^{+0.05137}_{-0.07393}$	$.46857^{+0.00888}_{-0.01307}$	$.4523^{+0.01291}_{-0.01129}$	$.42069^{+0.01107}_{-0.00919}$
Age/GYr	$13.733^{+0.389}_{-0.369}$	$13.908^{+0.399}_{-0.258}$	$14.408^{+0.369}_{-0.4}$	$15.338^{+0.342}_{-0.393}$
σ_8	$0.77^{+0.121}_{-0.109}$	$1.012^{+0.056}_{-0.081}$	$0.919^{+0.07}_{-0.075}$	$0.862^{+0.06}_{-0.063}$
τ	$0.095^{+0.072}_{-0.074}$	$0.047^{+0.037}_{-0.041}$	$0.079^{+0.023}_{-0.044}$	$0.081^{+0.024}_{-0.041}$

TABLE II: Most likely parameter values with 1σ errors for the various COSMOMC Runs

For the high multipoles ($31 \leq l \leq 1000$) TT power spectrum our goodness-of-fit (G.F.) is around 2%, compared to around 5% of the concordant Λ CDM model. For the overall fit of both the TT+TE+EE spectrum involving 3520 d.o.f., the EdS model has a reduced¹² $\chi_{eff,r}^2$ of 1.016 with a 26% G.F., as compared to the “concordance” Λ CDM model¹³ with $\chi_{eff,r}^2 = 1.005$ and G.F.=41% (see table IV for more details). The most likely parameter set along with

¹² The “effective” χ^2 is obtained directly from COSMOMC [16]. To obtain the reduced effective chi-square, $\chi_{eff,r}^2$, we just divide it with the number of independent degrees of freedom.

¹³ The “concordance” best fit Λ CDM model is obtained by running the COSMOMC program including both the WMAP 3-yr and supernovae data. The best-fit Λ CDM parameters for the WMAP 3-yr data alone yield very similar $\chi_{eff,r}^2$, indicating the presence of the well-known degeneracy in $\Omega_M - h$ plane of the WMAP data. In fact, it is this degeneracy that we exploit to fit CMB with $\Omega_M = 1$ and low Hubble parameter.

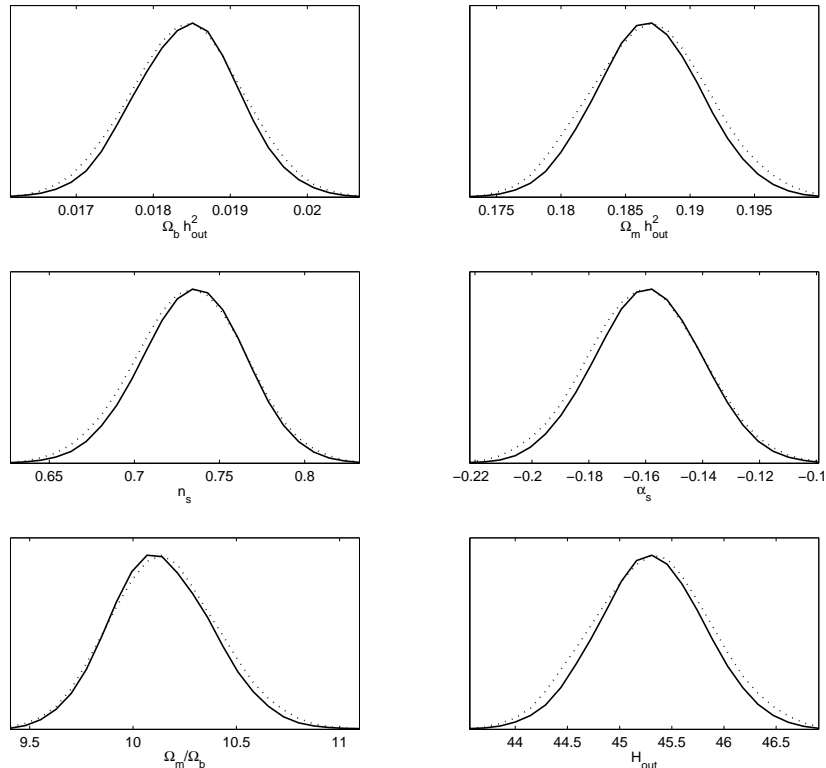


FIG. 5: Parameter likelihoods to the WMAP 3-yr data for the run “EdS, $\alpha_s \neq 0$ ”. Dotted lines are “mean likelihoods” of samples, while solid lines are “marginalized probabilities” [16].

their 1σ bounds are tabulated in table II; also see the likelihood plots, fig. 6.

We also produce two 2-dimensional likelihood contour plots: (i) h_{out} vs. Ω_m/Ω_b which are the only two independent parameters related to the composition of the universe, and (ii) n_s vs. α_s which characterize the spectrum.

The most crucial quantity to consider is the Hubble parameter and in particular what a consistency with the supernova data implies for the locally measured value. In fig. 7 we show a contour plot combining the constraint from supernova fit in the previous section with that of WMAP. As promised before, we find that the locally measured Hubble parameter can be as high as $h \sim .59$ at the 2σ , or 95% C.L., which is within the acceptable range of the different measurements of the Hubble parameter.

Let us briefly discuss about the values that we obtain for the other cosmological parameters, a more detailed discussion on some of these constraints is presented in the next section. The main constraint on the baryon density comes from BBN, and we are indeed consistent with the data (see next section for details). As one can see from the likelihood plot, fig. 6 as well as table II, the ratio between dark matter and baryons is somewhat higher, $\Omega_m/\Omega_b \sim 10$, than the “concordance” Λ CDM model value of $\Omega_m/\Omega_b \sim 6$. Measurements of light-to-mass functions in galaxy clusters can in principle be used to constrain these numbers, but presently they suffer from relatively large uncertainties (see for instance [44], and references therein). The issue is further compounded by the fact that our local ratio of abundances within the LTB patch may not represent the global ratio. A more detailed investigation will be required to settle the issue, but potentially this could be a problem. For the total matter density, one now has tight constraints from the observation of BAO [45]. As we discuss in the next section, the total matter density in our model (which is the same as the critical density and hence $\propto h_{\text{out}}^2$) seems consistent with these measurements.

What about the properties of the primordial spectrum? Our best fit spectral tilt is relatively low, $n_s \sim .73$, but there are several inflationary scenarios where such low spectral tilts are common (for example in modifications of the old inflationary scenario from false vacuum [48], or inflation from exponential potentials naturally occurring in string

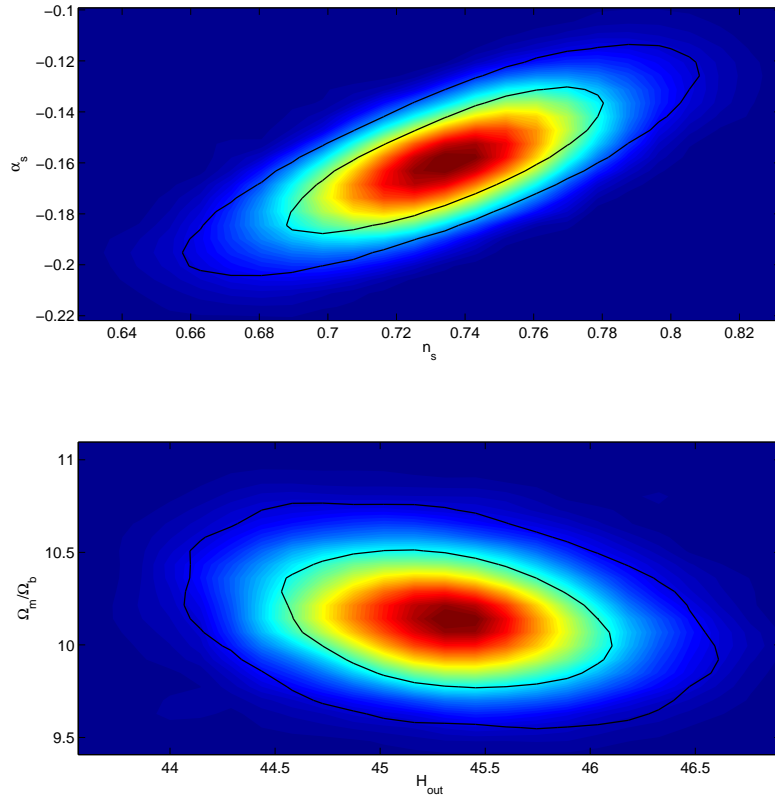


FIG. 6: Contour marginalized likelihood plots to the WMAP 3-yr data for the run “EdS, $\alpha_s \neq 0$ ”. The coloured map corresponds to mean likelihood, while the solid lines correspond to marginalized 1- σ and 2- σ contours.

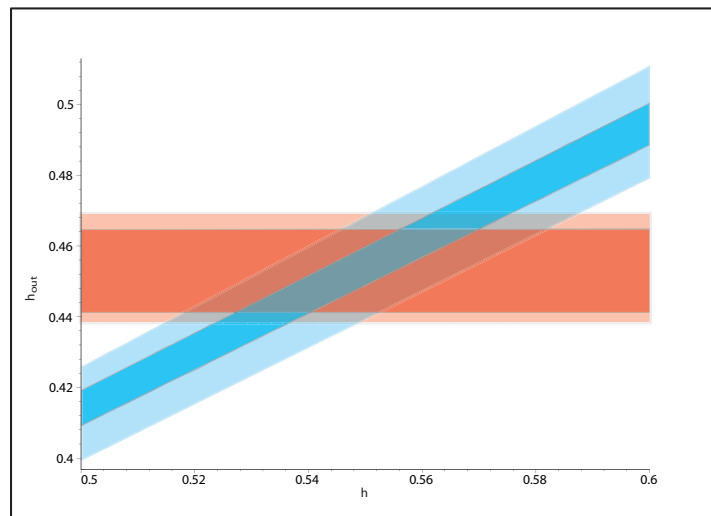


FIG. 7: 1- σ and 2- σ Contour plots for h vs. h_{out} . The blue bands come from the SN-I analysis, while the red bands correspond to constraints coming from WMAP.

Parameter	L	$\Omega_b h_{\text{out}}^2$	$\Omega_m h_{\text{out}}^2$	z_{re}	σ_8	n_s	α_s	δ_0	h_{out}	h
Best-fit	$250/h$	$0.018^{+0.002}_{-0.002}$	$0.19^{+0.01}_{-0.01}$	$13.8^{+2.2}_{-5.8}$	$0.92^{+0.07}_{-0.08}$	$0.73^{+0.07}_{-0.07}$	$-0.16^{+0.05}_{-0.04}$	$0.51^{+0.03}_{-0.04}$	$0.452^{+0.013}_{-0.011}$	$0.55^{+0.024}_{-0.023}$
Acceptable-fit	$160/h$	0.02	0.2	13.8	0.92	0.73	-0.16	0.44	0.47	0.55

TABLE III: Best-fit Minimal Void Model Parameters

theories, see for instance [49]). Our model also requires a significant running, $\alpha_s \sim -0.16$. It is a known fact that the 3rd year WMAP data favors a significant running of the spectral index which deviates from a Harrison-Zeldovich scale invariant scalar power spectrum. For example, the analysis of [50] gives a running $\alpha_s = -0.055^{+0.028}_{-0.029}$ at 60% confidence level. In fact, most inflationary models predict a running spectral index [51] (see also [52]; models of inflation from a False Vacuum have typically an abrupt transition in the spectral index [48]). Additional constraints on $\{n_s, \alpha_s, \sigma_8\}$ can mostly come from observations of large scale structure and weak-lensing experiments. In the context of our MV model, this is a difficult and somewhat tricky task which we have postponed to a future analysis, however we do discuss briefly possible implications in the next section.

Finally, we note that our value of the re-ionization epoch (optical depth) is broadly consistent with the usual observations [53] (see also discussion in [43]).

To summarize, our best fit (WMAP + SNIa) MV model consists of 8 parameters, one of which, the length scale of the void, has been chosen at the value $L = 250/h$ to derive our best-fit model. However, as noted in the introduction, if one “accepts” a G.F. $\sim 10\%$ to the supernovae data, then one can go down to a much smaller length scale, $L \sim 160/h$. Out of the other seven parameters, six of them (columns 2 to 7 in the Table of III are obtained from the fit to the WMAP 3-yr data using COSMOMC, while the last one, (column 8), is constrained from the supernovae data. We note that a “minimally acceptable” model with respect to the central underdensity contrast would be obtained with a maximally acceptable $h_{\text{out}} \sim 0.47$, at the 95% C.L.. This in conjunction with Eq.(1), then tells us that the minimal jump parameter has to be 1.17, or equivalently $\delta_0 \sim 0.44$. Using these information we tabulate all the parameters in Table III for our “best-fit” and “minimally-acceptable” model. We note that the values of δ_0 and L in the “minimally-acceptable” fit is not far from what observationally is suggested in [9].

VI. CAN WE IMPROVE WMAP AND SUPERNOVAE FITS?

We have seen that by allowing significant running in the range of the observed CMB spectrum one is able to obtain a reasonable fit to the WMAP 3yr data. However, the overall fit is not as good as the best-fit Λ CDM model. Secondly, as is clear from the combined contour plot fig. 7, consistency with WMAP and supernovae data requires a relatively low local value of the Hubble parameter. The underdensity contrast required is also quite high (centrally around 50%, and on average around 35% in the Void). Can we somehow modify the MV model to get a better fit and overcome these difficulties? We now discuss two different modifications in this context.

A. “Bump” Model

The first one concerns using different “priors” for the primordial spectrum. For instance, in [17] the authors assumed the existence of a bump in the primordial spectrum as a prior, rather than considering an overall running as we do, in order to fit the CMB data without Dark Energy. Although in these models the number of parameters is larger than what we consider, one obtains much better fits to the WMAP data (in fact, slightly better than Λ CDM), and is thus worth investigating further. Such a bump can be produced by a rapid succession of two phase transitions [17] and is thus phenomenologically well-motivated. Moreover, it is rather intriguing and promising to note that [18] such a bump would also enhance the probability of having voids today at the scale of the bump itself, which happens to be approximately the same scale we are considering here. This “bump” model, in its original form, of course cannot reproduce the supernovae data, and the Hubble parameter ($h_{\text{out}} \sim 0.44$) is too low. So it seems natural to merge this model with our MV scenario. Can the parameter set obtained be consistent with the supernovae analysis that we have performed using the local void?

Of course, having a local void again ensures that the supernovae data is consistent. The crucial question is whether putting together the MV framework with the “bump” model could lead to an “acceptable” local Hubble parameter. As we see in the contour plot (see fig. 8) at the 95% C.L. one can have as high as $h \sim .57$, which is definitely within

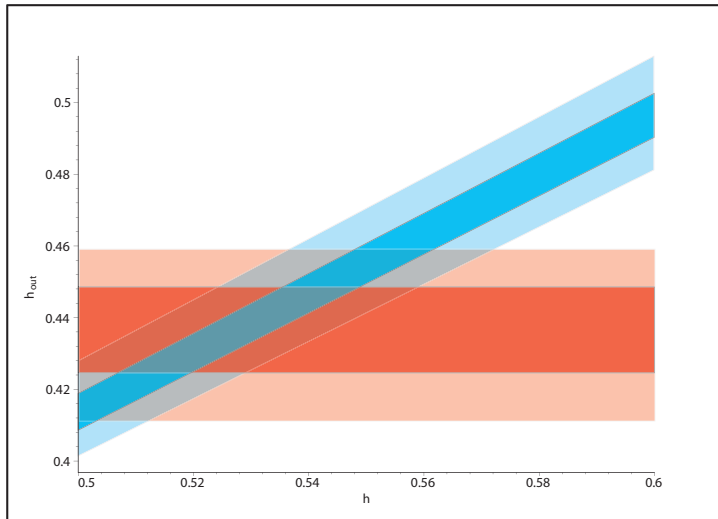


FIG. 8: $1\text{-}\sigma$ and $2\text{-}\sigma$ Contour plots for h vs. h_{out} for CDHM bump model [18]. The blue bands come from the SN-I analysis, while the red bands correspond to constraints coming from WMAP.

the acceptable range Eq.(1).

B. Adding Curvature

In this subsection we consider a different possibility, namely adding curvature to the model. Although having curvature would be considered fine-tuning in an inflationary paradigm, we point out that the low multipole anomalies [55], if taken seriously, could be suggestive of having only the “minimal” number (50-60 depending upon the reheating temperature) of efoldings, which would be consistent with having a slight curvature. Also, we note that other models involving cyclic scenarios typically do not predict a flat universe to any high precision.

Accordingly, we performed a run where we allowed up to 5% in curvature along with including running of the tilt, as before. We found that the best-fit parameter set prefers the highest value of spatial curvature that we allowed. Consequently, we performed a run with $\Omega_k = 0.05$, corresponding to a slightly closed universe to see how curvature may affect the goodness of fit¹⁴. We now indeed find a much better fit to the WMAP data. For the overall TT+TE+EE data, $\chi_{\text{eff},r}^2 = 1.012$ corresponding to a 31% goodness-of-fit (see table IV for more details). The Hubble parameter, however is slightly lower than our previous results, as can be seen from the likelihood plots involving (ii) Ω_k and h_{out} , also see table II. None of these results are very surprising or new. Previous studies had already observed that one can get good fits to WMAP with a closed universe, but it is precisely because of the rather low value of the Hubble parameter required for these fits that these models are not considered seriously. However, when combined with the jump parameter obtained from the supernovae analysis¹⁵ given by Eq.(10), this gives us a local Hubble parameter which can be consistent with observations, given in Eq.(1).

It is also worth pointing out that, as is clear from the contour plot fig. 9, there is a degeneracy direction in the WMAP data where as we simultaneously increase the curvature and the Hubble parameter we can still get good fits. This suggests that even if we allow for a slightly closed universe, by decreasing the Hubble parameter slightly (from our EdS value) we may be able to get significantly better fits to the WMAP data. In other words, when combined with other data, such as measurements of local Hubble parameter which prefer higher values of the Hubble parameter, the MV model may still provide a reasonable fit.

In passing we note that, the 2σ range for the tilt and the running is much closer to the conventional values as compared

¹⁴ We are currently pursuing a more exhaustive analysis of the void model with curvature.

¹⁵ In principle once one adds curvature, one has to redo the analysis of the supernovae data set. We have not done it for this preliminary analysis, because we do not expect any significant difference from the small amount of curvature that we allow.

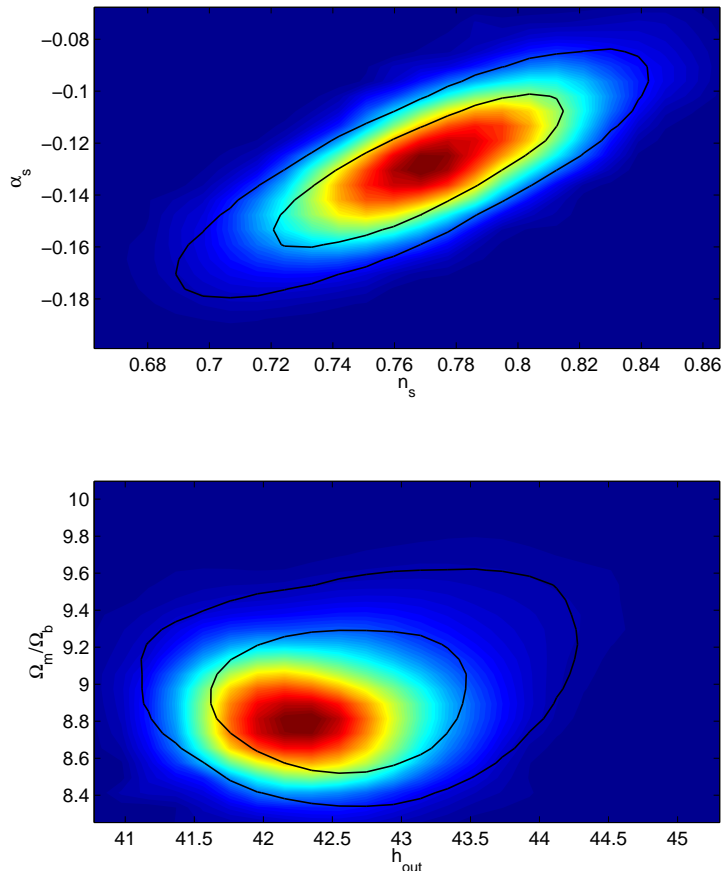


FIG. 9: Marginalized Likelihood plots for the WMAP 3-yr data for the run “EdS, α_s , $\Omega_k \neq 0$ ”. The coloured map corresponds to mean likelihood, while the solid lines correspond to marginalized $1\text{-}\sigma$ and $2\text{-}\sigma$ contours.

Model	C_l^{TT}		$C_l^{TT} + C_l^{TE}$		Total	
	χ_{eff}^2	G.F.	χ_{eff}^2	G.F.	χ_{eff}^2	G.F.
Concordant Λ CDM	1038.9	4.7%	1455.2	11.3%	3538.6	41%
EdS $\alpha_s = 0$	1124.6	0%	1711.9	0%	3652.3	6%
EdS $\alpha_s \neq 0$	1057.8	1.9 %	1475.5	5.7%	3577.4	24.6%
EdS α_s , $\Omega_k \neq 0$	1048.7	2.9%	1466	7.9%	3560.9	31.1%

TABLE IV: χ_{eff}^2 and goodness-of-fit for the different COSMOMC Runs. The first column corresponds to high- l TT power spectrum, ($31 \leq l \leq 1000$). The second column corresponds to both the high- l TT ($31 \leq l \leq 1000$) and TE ($24 \leq l \leq 450$) data. Finally, the last column contains the total statistics of TT ($2 \leq l \leq 1000$) and TE ($2 \leq l \leq 450$) spectrum.

to our original MV model (see figs. 6 and 9, for comparison).

VII. CONSISTENCY WITH OTHER OBSERVATIONS

Here we briefly discuss the consistency of our MV model with observations other than the supernovae, WMAP and local measurements of the Hubble parameter.

BBN: Primordial Nucleosynthesis has been a spectacular success story for the Standard Big Bang paradigm which

predicts specific freeze out abundances of light elements such as D , He^3 , He^4 and Li . These freeze out abundances depend on the baryon-to-photon ratio. Since from the measurements of CMB temperature we know the photon energy density precisely, BBN can also constrain the baryon density in our universe today. The success of the BBN paradigm lies in the general agreement of this number, measuring the abundances of the different light elements spanning 9 orders of magnitude (for a review see [54]). BBN therefore constrains the baryon density, so that at 95% C.L. we should have¹⁶ $0.017 \leq \Omega_b h_{\text{out}}^2 \leq 0.024$. This is indeed consistent with the parameter range that we obtain from the WMAP run, $\Omega_b h_{\text{out}}^2 = 0.018^{+0.002}_{-0.002}$. It is remarkable that although we have a higher baryonic abundance, the lower Hubble parameter almost precisely compensates to yield approximately the same baryonic energy density as it is obtained in the “concordance” Λ CDM model.

BAO: Recently, a remarkable achievement of observational cosmology has been to identify the baryon acoustic peak in the galaxy-galaxy correlation function using Luminous Red Galaxies (LRG’s) [45]. The overall shape of the galaxy correlation function mainly depends on the shape of the primordial spectrum (tilt and running) and the epoch of matter-radiation equality (scales which entered the Hubble horizon before the equality have their amplitudes relatively suppressed as compared to the ones which entered later). On top of the “overall envelope” one has now observed a tiny peak coming from the baryon acoustic oscillations. The position of the peak is related to the sound horizon of the baryon-photon plasma at the time of recombination. In fact, what one really measures is more like an angle which is the ratio of the sound horizon at recombination (evolved at $z \approx 0.35$, which is the average redshift of the LRG survey) and the angular distance¹⁷ at the same redshift $z \sim 0.35$. This ratio therefore is not only sensitive to the baryon density in the universe, but also to the evolution of our late-time universe and therefore, to the amount of dark energy, for instance. Using essentially the two pieces of information (overall shape and peak) one is able to constrain *two* different quantities, for instance, the matter density and d_V (a specific combination of the transverse and angular distance at $z \approx 0.35$ [45]). This in turn can constrain the composition of the universe and it was claimed in [45] that a pure EdS model is ruled out at the level of 5σ . Can the MV model be consistent?

Firstly, it is difficult to provide a crisp answer to that question based on the analysis done in [45] because the analysis of the data (conversion from redshift to distance etc.) is done using the “concordance” Λ CDM model. In particular we point out that precisely in the redshift range of the sample, $0.16 < z < 0.47$, the luminosity distance vs. redshift curve of the void model (which is the same as an EdS model, in this range) differs significantly from the Λ CDM curve. Thus to be precise, one needs to reanalyze the LRG data in the context of an EdS model. Nevertheless, one can try to see whether one can satisfy the bounds on d_V and $\Omega_m h^2$ that was placed in [45]:

$$d_V = 1370 \pm 128 \quad \text{and} \quad \Omega_m h^2 = 0.130 (n_s/0.98)^{1.2} \pm 0.022, \quad (17)$$

where the errors correspond to approximate 2σ (95% C.L.) values. Now, in our model, we have a low spectral tilt (and also a relatively large running, which can alter the shape of the correlation function and hence the constraints). Relegating a more systematic analysis for future, and just correcting for the lower tilt in our model implies the following constraint for the total matter density, which is given by the average Hubble parameter in our model:

$$\Omega_m h^2 \rightarrow h_{\text{out}}^2 = 0.185 \pm 0.022, \quad (18)$$

where we have used our best-fit spectral tilt, $n_s \approx 0.73$. We recall that our best fit Hubble parameter gives $h_{\text{out}}^2 \sim 0.205$, and therefore is consistent with the above bound.

On the other hand the angular distance at $z = 0.35$ for our model does not appear to be consistent with the values reported in [45]. In fact one can check that an EdS model has roughly the same distance of a concordance Λ CDM model at $z = 0.35$ if the ratio of the value of the Hubble constants of the two models is around 1.2. Since the concordance model (which fits the BAO scale) has $h \approx 0.7$, an EdS that fits this scale should have $h_{\text{out}} \approx 0.7/1.2 \approx 0.58$. As we have discussed, this value is too large with respect of our analysis of the WMAP data. More work is needed in order to find whether it would be possible to overcome this potential problem: for example adding more curvature could give a higher h_{out} , from WMAP (which, by the way, would make the whole scenario in better agreement with other data as well: for example with the local measurements of h). It has to be seen, through a combined statistical analysis including the BAO data, whether this could give a consistent picture. A different (though not very appealing) possibility, which would certainly work, is to make the Void much larger, extending up to redshifts of order $z \approx 0.4$.

¹⁶ While estimates from He^4 and D are slightly higher, measurements using Li suggests a lower number.

¹⁷ In the survey, one really measures a combination of the angular and transverse distances, see [45] for details.

We have checked that this can give the correct distance at $z \approx 0.35$ (see also the recent analysis in [46]), and that moreover this gives also a good fit of the BAO scale at $z \approx 0.2$, given in [47].

Observations from Large scale Structure and Weak lensing: An important class of cosmological observations comes from large scale structures and weak lensing observations. These typically produce constraints on σ_8 , as well as on the shape of the primordial spectrum, n_s and α_s (for instance using Lyman- α forest). However, as mentioned above, one has to revisit these analysis in the light of MV model, as one has a non-standard $D_L(z)$ relation. We leave for future such a careful study of the large scale structure, Lyman- α and weak lensing data. Let us still make a few brief comments.

About σ_8 , at first sight our value is a bit high, $\sigma_8 = 0.92^{+0.07}_{-0.08}$, in our model, but even if this situation turns out to be incompatible with the large-scale structure data (after a careful study), this may only be indicative of the need to include some hot dark matter component [17, 18]. In the light of neutrinos having mass, this is a perfectly natural scenario to consider. About n_s and $|\alpha_s|$, the values are respectively lower and higher than what the conventional Λ CDM analysis suggests and in particular one may worry about conflicts with Lyman- α measurements. However, we firstly point out that an analysis of the Lyman- α measurements has to be now re-done in combination with the different set of priors that we use to study the WMAP data. Secondly, introducing new physics, such as including a little curvature, can push the values of n_s and α_s much closer to the standard values. In short, there are too many uncertainties for us to make here any concrete conclusions, and one really needs to perform a careful study of the above mentioned observations.

ISW Correlations: Another interesting piece of evidence for Dark energy is given by the Integrated Sachs Wolfe effect, which is claimed to be detected with some significance by some collaborations [40]. The detection is a correlation between the CMB maps of the sky and the galaxy surveys, which cannot be explained in an EdS universe (since in this case the linear gravitational potential does not evolve and therefore CMB photons do not get any net frequency shift when passing through a potential well), and therefore are interpreted as independent evidence for Dark Energy (since the potentials can evolve in Λ CDM). However the effect is absent only at the linear level, and it exists also in EdS in the presence of nonlinear gravitational clustering. This is usually assumed to be smaller than 10^{-5} , but it actually happens to be of order 10^{-5} (and thus, visible in the CMB) for structures as large as those that we are proposing in the present paper (few hundreds of Mpc). It would be interesting to try and reproduce the ISW detection assuming the presence of large voids and structures in the sky.

Moreover in the local underdense region we have assumed that the growth of fluctuations is different than the flat CDM model (it is in fact more similar to an open Universe): this leads also to an ISW effect for density fluctuations localized inside the Void. Studying this effect would be very interesting and could significantly affect the low- l part of the CMB spectrum and therefore also the parameter estimation from the CMB. However this goes beyond the scope of the present paper since it would require a full treatment of the growth of density fluctuations in an LTB metric (this problem has been recently attacked by [59]).

VIII. CONCLUSION AND DISCUSSION

The Type Ia supernovae data reveal that our universe is accelerating at redshifts that approximately correspond to the epoch of non-linear structure formation on large scales (the epoch of the formation of the so-called “cosmic web”). Given this fact, we have explored the possibility that the effect of a large scale void can account for this acceleration due to a jump between the local and the average Hubble parameter, instead of invoking a spatially constant dark energy/cosmological constant component. We find that the Minimal Void (MV) model can consistently account for the combination of the Type Ia supernovae, WMAP 3rd year, BBN constraints, provided that the void spans a radius of about of 200 Mpc/ h with a relative under density of 45%, near the center. The MV model can accommodate reasonably all of the data considered, although the fits are not as good as the concordance model. However, we see the possibility of obtaining just as good fits when one includes curvature or invokes non-standard features in the primordial spectrum (a “bump” for example). We leave these issues for an upcoming work. On the other hand we have seen that the Minimal Void is in trouble with the Baryon Acoustic Oscillations measurements, since outside the Void, the $D_L(z)$ curve is just the usual EdS one, and the Hubble parameter h_{out} from WMAP is too low. More work is needed in order to find whether it would be possible to overcome this potential problem (for example by finding a fit for WMAP with higher h_{out}).

We end with observational and theoretical possibilities of distinguishing the MV model from Λ CDM. The MV model predicts that the spectral index has to run significantly in the WMAP3 data and that the “average” Hubble constant (*i.e.* outside the local region) has to be around $h_{\text{out}} \sim 0.45$. The Λ CDM model, instead, requires a finely

tuned cosmological constant or dark energy component, in order to be consistent with the same data set. Both cases require significant model building and new physics that are currently being pursued by the community. How are we to distinguish between these two models? The first logical way seems to perform galaxy counts up to very large distances and in a wide area in the sky, in order to directly check if we could really live inside a huge Void. Moreover, there are features which can be checked by looking at SN Ia themselves: firstly, the luminosity-redshift curve in the two models deviate from each other significantly at redshifts $z \geq 1$. Secondly, in the MV model the curve has a sharp peak (in correspondence with the boundary of the local region) around $z \simeq 0.1$, while this peak does not exist in the Λ CDM model. The up-coming experiment SDSS-II [30] will probably be able to discriminate the presence of such a peak. Another unique prediction for the MV model comes from realizing that the void is not expected to be exactly spherically symmetric, which could lead to detectable anisotropies in the Hubble parameter as well as in the low multipoles in CMB. Additionally, these anisotropies should be correlated! We note, also, that one could be able to constrain Voids by looking at the blackbody nature of the CMB [56, 57]. Our MV is still consistent with these constraints (while, according to [57], voids that extend up to $z \sim 1$ are excluded). Finally, studying large scale structure (as we plan to do in future work) one can study the compatibility of the primordial power spectrum we are assuming (with low tilt and large running, or with a bump) with the matter power spectrum. It may also be possible to test the existence of such a large running using Planck-satellite data as suggested by the Bayesian analysis performed in [58] using simulations.

In conclusion, we have shown that, for WMAP and SNIa observations, the MV model could be taken as an alternative to invoking a dark energy component that will be further tested in forthcoming supernovae observations. On the other hand this has to be made consistent also with the Baryon Acoustic Oscillations. On the theoretical end, much work needs to be done to establish if such large voids can actually be produced in our Universe by generic physics of structure formation. We are currently pursuing this issues.

Note Added: Most of the above research work was completed before the release of the WMAP 5yr data and we have decided not to re-analyze the CMB data in the present paper for the following reason: although the 5-yr data improves the 3-yr data, there is no significant qualitative difference between the results presented in the 3-yr and 5-yr survey. In this context, we further emphasize that our aim in this manuscript is not to compete with Λ CDM on the basis of Bayesian likelihood analysis (in which case the analysis can be very sensitive to the data, for instance a difference of $\chi^2 \sim 1 - 2$ may be significant), but to simply present a model which can be consistent with the data on the basis of the goodness of fit (for instance, a difference of $\chi^2 \sim 1 - 2$ does not significantly reduce the goodness of fit). In addition a more systematic treatment including other cosmological data (BAO, Large Scale Structure data) and more recent data (CMB and Supernovae) is the subject of a future publication.

Acknowledgments

We would like to thank Robert Brandenberger, Paul Hunt, Subir Sarkar, Ravi Seth and Tarun Souradeep, for useful discussions and suggestions. We would specially like to thank Suman Bhattacharya, Jason Holmes and Antony Lewis for their help with COSMOMC. We thank Sebastian Szybka and Seshadri Nadathur for pointing out typos in earlier versions of the manuscript.

IX. APPENDICES: ANALYTICAL RESULTS FOR LTB METRIC

A. Metric & Density Profile

In our paper we are interested in a special class of exact spherically symmetric solutions of Einstein's equations with dust, known as the "open" LTB metric (in units $c = 1$). We follow the treatment given in ([3, 34]), where we have set the "mass function" to be cubic, which amounts to a redefinition of the radial coordinate (which is always possible if the mass function is a growing function of r). The metric is given by:

$$ds^2 = -dt^2 + S^2(r, t)dr^2 + R^2(r, t)(d\theta^2 + \sin^2\theta d\varphi^2), \quad (19)$$

Here we have employed comoving coordinates (r, θ, φ) and proper time t . The functions $S^2(r, t)$ and the dust density $\rho(r, t)$ is given in terms of $R(r, t)$ via

$$S^2(r, t) = \frac{R'^2(r, t)}{1 + 2(Mr)^2 k(r)}, \quad (20)$$

$$\rho(r, t) = \frac{\bar{M}^2 M_p^2 r^2}{R'(r, t) R^2(r, t)}, \quad (21)$$

where a dot denotes partial differentiation with respect to t and a prime with respect to r , while the function $R(r, t)$ itself is given implicitly as a function of (r, t) via an auxiliary variable $u(r, t)$:

$$R(r, t) = \frac{2\pi r}{3k(r)} (\cosh u - 1), \quad (22)$$

$$\tau^3 \equiv \bar{M}t = \frac{\pi\sqrt{2}}{3k(r)^{3/2}} (\sinh u - u), \quad (23)$$

In the above expressions, the ‘‘curvature’’ function $k(r)$ is left arbitrary (except that $k(r) \geq 0$) and this is what controls the density profile inside the LTB patch, while M is just an arbitrary (unphysical) mass scale. Also, we have introduced the dimensionless conformal time τ for later convenience.

We also note that the average density inside the LTB patch is equal to the outside FLRW density (see for instance [3, 34]), in the limit in which we can neglect $(Mr)^2 k(r)$ in Eq.(20) in the spatial metric when defining the average (in our case the correction is always negligible).

To get an intuitive and analytical understanding of how the density profile is related to the curvature function it is instructive to look at the ‘‘small- u ’’ approximation where we only keep next-to-leading terms in Eq.(22) and Eq.(23). This gives us Eq.(2).

B. Photon Trajectories

In order to perform supernovae fits we need to compute the luminosity (or angular) distances and redshifts for a photon trajectory emanating (backwards in time) from the central observer. The first step in this direction is to solve for the photon trajectory:

$$ds^2 = 0 \Rightarrow \frac{dt(r)}{dr} = -\frac{R'(r, t(r))}{\sqrt{1 + 2(Mr)^2 k(r)}}. \quad (24)$$

The negative sign in front takes care of the fact that the time increases as the photons go towards the center. Analytical progress in solving the above equation is possible by realizing two things. Firstly, all quantities $(t(r), z(r), D_L(r))$ can be expressed as a power series in, $\bar{M}r \sim r/R_H$, and since this is a small quantity for the relevant inhomogeneous patches, we can just keep the next-to-leading order terms in these expansions [34]. Secondly, formally one can combine Eq.(22) and Eq.(23) to give us a power series expansion for $R(r, t)$ explicitly in terms of (r, t) [34]:

$$R(r, t) = \frac{1}{3}\pi\gamma^2 r\tau^2 (1 + R_2 u_0^2 + R_4 u_0^4 + \dots) \equiv \frac{1}{3}\pi\gamma^2 r\tau^2 (1 + f(u_0^2)), \quad (25)$$

where

$$u_0 \equiv \gamma(\bar{M}t)^{1/3} \sqrt{k(r)} \quad \text{and} \quad \gamma \equiv \left(\frac{9\sqrt{2}}{\pi}\right)^{1/3}. \quad (26)$$

It is important to realize that the coefficients $\{R_n\}$, and hence the function f are universal (do not depend on the specific curvature function). It is implicitly defined via

$$1 + f(u_0^2) \equiv \frac{2(\cosh u - 1)}{u_0^2} \quad \text{and} \quad 6(\sinh u - u) = u_0^3. \quad (27)$$

This is what allows us to analyze the problem in its full generality.

It is convenient to recast the equation in terms of the conformal time, τ , and the dimensionless radial coordinate

$$\bar{r} = \bar{M}r. \quad (28)$$

Substituting Eq.(25) in Eq.(24) one finds

$$\frac{d\tau}{d\bar{r}} = -\frac{\frac{\pi}{9}\gamma^2 [1 + \sum_1^\infty R_{2n}\gamma^{2n}\tau^{2n}(\bar{r}k^n)']}{\sqrt{1 + 2k\bar{r}^2}}. \quad (29)$$

The prime now denotes differentiation with respect to the rescaled \bar{r} . This can now be solved perturbative in \bar{r} to give us

$$\tau = \left(\tau_0 - \frac{\pi}{9}\gamma^2\bar{r}\right) - \frac{\pi}{9}\gamma^2\bar{r} \sum_1^\infty R_{2n}\gamma^{2n}\tau_0^{2n}k^n(\bar{r}) + \mathcal{O}(\bar{r}^2). \quad (30)$$

The first two terms within the brackets corresponds to the FLRW expression for the trajectory while the rest of the terms give us the largest corrections coming from the inhomogeneities within a local patch. For corrections outside the patch see [34]. By comparing with Eq.(25) the above expression can succinctly be written as

$$\tau(\bar{r}) = \tau_F(\bar{r}) - \frac{\pi}{9}\gamma^2\bar{r}f(\gamma^2\tau_0^2k(\bar{r})), \quad (31)$$

where the subscript F corresponds to FLRW.

C. Luminosity Distance vs. Redshift

Having found the photon trajectory, the next step is to compute the redshift which is governed by the differential equation [2]

$$\frac{dz}{dr} = \frac{(1+z)\dot{R}'}{\sqrt{1 + 2k\bar{r}^2}}. \quad (32)$$

Again, if we are only interested in computing corrections up to linear order in \bar{r} , then the redshift is given by

$$\int \frac{dz}{1+z} \approx \frac{2\pi\gamma^2}{9} \int \frac{d\bar{r}}{\tau} [1 + \sum_n (n+1)R_n\gamma^{2n}\tau^{2n}(rk^n)'] = \frac{2\pi\gamma^2}{9} \int \left[\frac{d\bar{r}}{\tau} + d\bar{r} \sum_n (n+1)R_n\gamma^{2n}\tau^{2n-1}(rk^n)' \right]. \quad (33)$$

To evaluate the first integral we note that we can replace τ by τ_F as we will only be making an $\mathcal{O}(\bar{r}^2)$ error. Thus we have

$$\int \frac{d\bar{r}}{\tau} \approx \int \frac{d\bar{r}}{\tau_F} = -\frac{9}{\pi\gamma^2} \int \frac{d\tau_F}{\tau_F} = -\frac{9\gamma^2}{\pi} \ln \frac{\tau_F}{\tau_0}$$

The second term can be integrated straight forwardly up to linear terms in \bar{r} :

$$\begin{aligned} \sum_n (n+1)R_n\gamma^{2n} \int \tau^{2n-1}(rk^n)' d\bar{r} &\approx \sum_n (n+1)R_n\gamma^{2n}\tau_0^{2n-1} \int (\bar{r}k^n)' d\bar{r} = \sum_n (n+1)R_n\gamma^{2n}\tau_0^{2n-1}\bar{r}k^n \\ &= \bar{r}[f(\gamma^2\tau_0^2k(r)) + \gamma^2\tau_0^2k(r)f_1(\gamma^2\tau_0^2k(r))]/\tau_0 \end{aligned}$$

where we have defined

$$f_1(x) \equiv \frac{df(x)}{dx} \quad (34)$$

Putting everything together we have

$$1+z = \left[\frac{\tau_0}{\tau_F(\bar{r})} \right]^2 \exp \left\{ \frac{2\pi\gamma^2\bar{r}[f(\gamma^2\tau_0^2k(r)) + \gamma^2\tau_0^2k(r)f_1(\gamma^2\tau_0^2k(r))]}{9\tau_0} \right\}. \quad (35)$$

Thus we have obtained an analytical approximation for the redshift as a function of the radial coordinate. We note in passing that the term in front of the exponential precisely correspond to the FLRW result. The corrections come from the exponential. In fact for small z one finds

$$z \approx \frac{2\pi}{9\tau_0} \gamma^2 \bar{r} [1 + f(\gamma^2 \tau_0^2 k(r)) + \gamma^2 \tau_0^2 k(r) f_1(\gamma^2 \tau_0^2 k(r))]. \quad (36)$$

The luminosity distance, in General Theory of Relativity, is related to the angular diameter distance, D_A via

$$D_L = (1 + z)^2 D_A. \quad (37)$$

Now, in an LTB model when the observer is sitting at the center, the angular distance is simply given by

$$D_A = R = \frac{1}{3} \pi \gamma^2 r \tau^2 (1 + f(\gamma^2 \tau_0^2 k(\bar{r}))). \quad (38)$$

Thus we now have both the luminosity distance and the redshift as a function of the radial coordinate and one can easily plot $D_L(z)$ and check whether the local void model can provide a good fit to the supernova data or not.

D. The “Jump”

A particularly important quantity that can be inferred from the $D_L(z)$ curve is the jump parameter, \mathcal{J} defined by Eq.(9). Surprisingly, this turns out to not depend on the specific profiles, let us here see this analytically. First observe that since k' vanishes at $r = 0$, we have the general result

$$R'(0, t) = \frac{1}{3} \pi \gamma^2 \tau_0^2 (1 + f_0), \quad (39)$$

where f_0 corresponds to the value of f at $r = 0$. Then using the exact expression for the density function Eq.(21) one finds

$$\rho(r, t) = \frac{M_p^2}{6\pi t_0^2 (1 + f_0)^3}. \quad (40)$$

The underdensity contrast at the center, δ_0 now can be easily related to f_0 :

$$\delta_0 = (1 + f_0)^{-3} - 1 \Rightarrow 1 + f_0 = (1 + \delta_0)^{-1/3}. \quad (41)$$

Now, on the other hand using the definition of the Hubble parameter Eq.(8), the correction to the redshift Eq.(36), and the luminosity distance Eq.(38) one finds

$$H_0^{-1} = H_{\text{out}}^{-1} \frac{1 + f_0}{1 + f_0 + u_0^2 f_{1,0}}.$$

Or in other words

$$\mathcal{J} = \frac{h}{h_{\text{out}}} = \frac{1 + f_0 + u_0^2 f_{1,0}}{1 + f_0}. \quad (42)$$

Since δ_0 uniquely determines f_0 via (41), and $f(u_0^2)$ is a given function, it also determines u_0^2 and $f_{1,0} \equiv f_1(u_0^2)$. Thus in turn it also determines the jump parameter uniquely.

E. CMB dipole moment

Let us consider our observer to be located slightly off-center, at $r = r_O$. In this case the non-zero radial velocity of the observer will contribute towards a dipole moment in CMB:

$$\frac{\delta T}{T} \sim v_O = \dot{d}_O, \quad (43)$$

where the proper radial distance, d_O , of the observer is given by

$$d_O = \int_0^{r_O} dr \frac{R'}{\sqrt{1 + 2(Mr)^2 k(r)}}$$

Now, in our profile $k(r)$ remains almost a constant for almost the entire underdense region. Assuming we are living in this “constant” underdense region, we have

$$d_O = \frac{2\pi(\cosh u - 1)}{3k_{\max}} \int_0^{r_O} \frac{dr}{\sqrt{1 + 2(Mr)^2 k_{\max}}} = \frac{2\pi(\cosh u - 1) \sinh^{-1}(\bar{M}\sqrt{2k_{\max}}r_O)}{3k_{\max}\bar{M}\sqrt{2k_{\max}}}$$

(The simplification occurs because u and hence R' becomes only a function of time.) Further, since $\bar{M}r_O$ is expected to be very small, we have

$$d_O = \frac{2\pi(\cosh u - 1)r_O}{3k_{\max}}. \quad (44)$$

Taking the time derivative and simplifying we find

$$\dot{d}_O = \frac{d_O H_{\text{out}}}{4} \frac{u_0^3 \sinh u}{(\cosh u - 1)^2}. \quad (45)$$

We now note that $u(u_0)$ is a known function Eq.(27), in turn u_0 is known in terms of δ_0 via the function $f(u_0^2)$, see Eq.(41). Thus, in principle, the second term in the right hand side of Eq.(45) is determined in terms of the central underdensity contrast. Also, since the measured value of the CMB dipole moment $\sim 10^{-3}$, naturalness arguments suggest \dot{d}_O to be of the same order, and thus we have (after some simplifications):

$$d_O H_{\text{out}} \sim 10^{-3} \frac{\sqrt{2}(1 + f_0)^2}{\sqrt{u_0^2(1 + f_0)^2 + 2(1 + f_0)}}. \quad (46)$$

For voids of around $200/h$ Mpc, and central underdensity contrasts between 40% and 50%, the dipole constraint Eq.(46) typically imply that “we” have to be located within 10% of the void radius.

F. Analytic expression for the $D_L - z$ curve

In this subsection we wish to provide the reader a self-consistent summary of all the equations which are needed to plot the $D_L - z$ curve, in an analytic form. Following this, a fit of any experimental dataset can easily be performed. Here is the set of equations, which give D_L and z as a function of the radial coordinate r (therefore implicitly $D_L - z$). First of all one needs to define the function $f(u_0^2)$, implicitly given by:

$$f \equiv \frac{\sqrt[3]{2}(\cosh(u) - 1)}{3^{2/3}(\sinh(u) - u)^{2/3}} - 1 \quad (47)$$

$$u_0 = 6^{1/3}(\sinh(u) - u)^{1/3}. \quad (48)$$

Then, one can use this function in the following equations:

$$\tau(r) = \tau_0 - \frac{\pi}{9}\gamma^2 \bar{M}r[1 + f(\gamma^2 \tau_0^2 k(r))], \quad (49)$$

$$1 + z(r) = \left(\frac{\tau_0}{\tau(r)}\right)^2 \exp\left[\frac{4\pi\gamma^2 \bar{M}r}{9}f(\gamma^2 \tau_0^2 k(r))\right] \quad (50)$$

$$D_L(r) = \frac{\pi}{3}\gamma^2 r \tau(r)^2 [1 + f(\gamma^2 \tau_0^2 k(r))] [1 + z(r)]^2 \quad (51)$$

$$\tau_0 = \left(\frac{2\bar{M}}{3H_{\text{out}}}\right)^{1/3} \quad (52)$$

$$\gamma = \left(\frac{9\sqrt{2}}{\pi}\right)^{1/3} \quad (53)$$

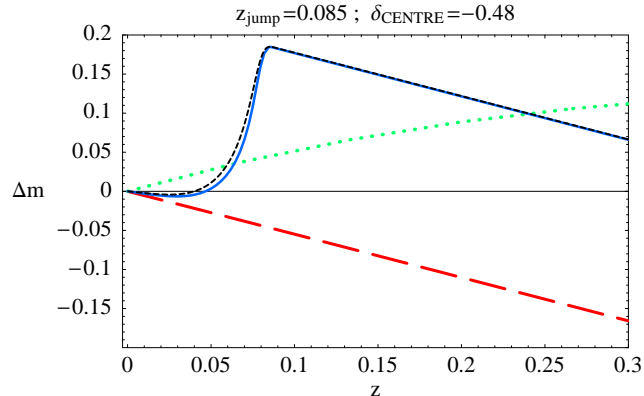


FIG. 10: Comparison between analytic and numerical $D_L - z$ curves. The numerical curve is the blue solid line, the analytic approximation is the black short-dashed line. We have plotted also the EdS curve (red long-dashed line) and the Λ CDM, with $\Omega_\Lambda = 0.7$ (green dotted line). We have used the value $L = 400$, with the units given in Eq. (55), and $k_{\max} = 2.2$ (which corresponds to a density contrast at the center $\delta_0 = -0.25$).

The above formulas are completely general for any LTB profile, but we now focus into our specific one given by

$$k(r) = k_{\max} \left[1 - \left(\frac{r}{L} \right)^4 \right]^2. \quad (54)$$

Then one has to choose appropriate values for H_0 , and for the length units for the coordinate r (given by \bar{M}). A simple choice is to set:

$$\sqrt{\frac{8\pi}{3}} \bar{M} = H_{\text{out}} = h_{\text{out}}/3000, \quad (55)$$

where we have chosen, in this way, the units $\text{Mpc}=1$ (which turns out to be a convenient choice for the problem). Once this is done the physical parameter L (the radius of the patch) is approximately given already in Mpc. The comparison between the obtained curve and the fully numerical curve is shown in fig. (10)

Finally the reader may play with the two parameters: the size L and k_{\max} (which sets the amplitude of the density contrast). We also recall that the density profile is given by Eq.(2) and that k_{\max} can be directly related to the density contrast δ_0 at the center of the void at the present time, via the following equation:

$$\delta_0 = [1 + f(\gamma^2 \tau_0^2 k_{\max})]^{-3} - 1. \quad (56)$$

-
- [1] K. Tomita, arXiv:astro-ph/9906027, Mon. Not. Roy. Astron. Soc. **326**, 287 (2001) [arXiv:astro-ph/0011484], and Prog. Theor. Phys. **106**, 929 (2001) [arXiv:astro-ph/0104141], and Astrophys. J. **529** (2000) 38 [arXiv:astro-ph/9906027] and Prog. Theor. Phys. **108** (2002) 103 [arXiv:astro-ph/0203125];
J. W. Moffat, JCAP **0510**, 012 (2005) astro-ph/0502110 and JCAP **0605**, 001 (2006); R. Mansouri, arXiv:astro-ph/0512605; H. Alnes, M. Amarzguioui and O. Gron, Phys. Rev. D **73**, 083519 (2006) [arXiv:astro-ph/0512006]; D. J. H. Chung and A. E. Romano, Phys. Rev. D **74**, 103507 (2006) [arXiv:astro-ph/0608403].
- [2] M. N. Celerier, Astron. Astrophys. **353**, 63 (2000) [arXiv:astro-ph/9907206].
- [3] T. Biswas, R. Mansouri and A. Notari, arXiv:astro-ph/0606703.
- [4] M. N. Celerier, arXiv:astro-ph/0702416.
- [5] S. F. Shandarin, J. V. Sheth and V. Sahni, Mon. Not. Roy. Astron. Soc. **353**, 162 (2004) [arXiv:astro-ph/0312110].
- [6] J. R. I. Gott *et al.*, Astrophys. J. **624**, 463 (2005) [arXiv:astro-ph/0310571].
- [7] J. Einasto, arXiv:astro-ph/0609686.
- [8] P. J. E. Peebles, arXiv:astro-ph/0101127.
- [9] W. J. Frith, G. S. Buswell, R. Fong, N. Metcalfe and T. Shanks, Mon. Not. Roy. Astron. Soc. **345**, 1049 (2003) [arXiv:astro-ph/0302331].

- [10] M. Cruz, M. Tucci, E. Martinez-Gonzalez and P. Vielva, *Mon. Not. Roy. Astron. Soc.* **369** (2006) 57 [arXiv:astro-ph/0601427]. M. Cruz, L. Cayon, E. Martinez-Gonzalez, P. Vielva and J. Jin, *Astrophys. J.* **655** (2007) 11 [arXiv:astro-ph/0603859].
- [11] L. Rudnick, S. Brown and L. R. Williams, arXiv:0704.0908 [astro-ph].
- [12] K. T. Inoue and J. Silk, arXiv:astro-ph/0612347; K. T. Inoue and J. Silk, arXiv:astro-ph/0602478.
- [13] D. J. Schwarz and B. Weinhorst, arXiv:0706.0165 [astro-ph].
- [14] M. L. McClure and C. C. Dyer, *New Astron.* **12**, 533 (2007) [arXiv:astro-ph/0703556].
- [15] K. Tomita, *Prog. Theor. Phys.* **105**, 419 (2001) [arXiv:astro-ph/0005031].
- [16] A. Lewis and S. Bridle, *Phys. Rev. D* **66**, 103511 (2002) [arXiv:astro-ph/0205436]; <http://cosmologist.info/cosmomc/>.
- [17] P. Hunt and S. Sarkar, arXiv:0706.2443 [astro-ph].
- [18] A. Blanchard, M. Douspis, M. Rowan-Robinson and S. Sarkar, *Astron. Astrophys.* **412**, 35 (2003) [arXiv:astro-ph/0304237].
- [19] A. Shafieloo and T. Souradeep, arXiv:0709.1944 [astro-ph].
- [20] S. Nobbenhuis, *Found. Phys.* **36**, 613 (2006) [arXiv:gr-qc/0411093].
- [21] G. Lemaitre, *Ann. soc. Sci. Bruxelles Ser.1*, A53, 51, 1933; R. C. Tolman, *Proc. Natl. Acad. Sci. U.S.A.* 20,410, 1934; H. Bondi, *Mon. Not. R. Astron. Soc.*, 107, 343, 1947).
- [22] S. Khakshournia and R. Mansouri, *Gen. Rel. Grav.* **34**, 1847 (2002) [arXiv:gr-qc/0308025].
- [23] Y. B. Zeldovich, *Astron. Astrophys.* **5** (1970) 84.
- [24] V. Marra, E. W. Kolb, S. Matarrese and A. Riotto, arXiv:0708.3622 [astro-ph]; V. Marra, E. W. Kolb and S. Matarrese, arXiv:0710.5505 [astro-ph].
- [25] N. Brouzakis, N. Tetradis and E. Tzavara, *JCAP* **0702**, 013 (2007) [arXiv:astro-ph/0612179]; N. Brouzakis, N. Tetradis and E. Tzavara, arXiv:astro-ph/0703586.
- [26] K. Enqvist and T. Mattsson, *JCAP* **0702**, 019 (2007) [arXiv:astro-ph/0609120]; K. Enqvist, arXiv:0709.2044 [astro-ph].
- [27] G. M. Hossain, arXiv:0709.3490 [astro-ph].
- [28] D. L. Wiltshire, gr-qc/0503099; D. L. Wiltshire, *New J. Phys.* **9**, 377 (2007) [arXiv:gr-qc/0702082]; D. L. Wiltshire, *Phys. Rev. Lett.* **99**, 251101 (2007) [arXiv:0709.0732 [gr-qc]]; B. M. Leith, S. C. C. Ng and D. L. Wiltshire, *Astrophys. J.* **672**, L91 (2008) [arXiv:0709.2535 [astro-ph]].
- [29] A. G. Riess *et al.*, arXiv:astro-ph/0611572. Data available at <http://braeburn.pha.jhu.edu/~ariess/R06/>
- [30] <http://sdssdp47.fnal.gov/sdssn/sdssn.html>
- [31] S. Jha, A. G. Riess and R. P. Kirshner, *Astrophys. J.* **659**, 122 (2007) [arXiv:astro-ph/A. Conley, R. G. Carlberg, J. Guy, D. A. Howell, S. Jha, A. G. Riess and M. Sullivan, arXiv:0705.0367 [astro-ph].
- [32] S. Perlmutter *et al.* [Supernova Cosmology Project Collaboration], *Astrophys. J.* **517**, 565 (1999) [arXiv:astro-ph/9812133]; A. G. Riess *et al.* [Supernova Search Team Collaboration], *Astron. J.* **116**, 1009 (1998) [arXiv:astro-ph/9805201]. A. G. Riess *et al.* [Supernova Search Team Collaboration], *Astrophys. J.* **607**, 665 (2004) [arXiv:astro-ph/0402512].
- [33] S. M. Carroll, W. H. Press and E. L. Turner, *Ann. Rev. Astron. Astrophys.* **30**, 499 (1992).
- [34] T. Biswas and A. Notari, arXiv:astro-ph/0702555.
- [35] B. R. Parodi, A. Saha, A. Sandage and G. A. Tammann, arXiv:astro-ph/0004063.
- [36] W. L. Freedman *et al.*, *Astrophys. J.* **553**, 47 (2001) [arXiv:astro-ph/0012376].
- [37] A. Sandage, G. A. Tammann, A. Saha, B. Reindl, F. D. Macchetto and N. Panagia, *Astrophys. J.* **653**, 843 (2006) [arXiv:astro-ph/0603647].
- [38] E. D. Reese, J. E. Carlstrom, M. Joy, J. J. Mohr, L. Grego and W. L. Holzapfel, *Astrophys. J.* **581**, 53 (2002) [arXiv:astro-ph/0205350]; J. E. Carlstrom, G. P. Holder and E. D. Reese, *Ann. Rev. Astron. Astrophys.* **40**, 643 (2002) [arXiv:astro-ph/0208192].
- [39] C. S. Kochanek and P. L. Schechter, arXiv:astro-ph/0306040.
- [40] P. Fosalba, E. Gaztanaga and F. Castander, *Astrophys. J.* **597** (2003) L89 [arXiv:astro-ph/0307249]. S. Boughn and R. Crittenden, *Nature* **427** (2004) 45 [arXiv:astro-ph/0305001]. T. Giannantonio *et al.*, *Phys. Rev. D* **74** (2006) 063520 [arXiv:astro-ph/0607572]. D. Pietrobon, A. Balbi and D. Marinucci, *Phys. Rev. D* **74**, 043524 (2006) [arXiv:astro-ph/0606475]. J. D. McEwen, P. Vielva, M. P. Hobson, E. Martinez-Gonzalez and A. N. Lasenby, *Mon. Not. Roy. Astron. Soc.* **373** (2007) 1211 [arXiv:astro-ph/0602398]. *Mon. Not. Roy. Astron. Soc.* **377**, 1085 (2007) [arXiv:astro-ph/0610911].
- [41] J. M. H. Etherington, *Phil. Mag.* **15**, 761 (1933); G. F. R. Ellis, in *Proc. School "Enrico Fermi"*, Ed. R. K. Sachs, New York (1971).
- [42] H. Alnes and M. Amarguioui, *Phys. Rev. D* **74**, 103520 (2006) [arXiv:astro-ph/0607334].
- [43] D. N. Spergel *et al.* [WMAP Collaboration], *Astrophys. J. Suppl.* **170**, 377 (2007) [arXiv:astro-ph/0603449].
- [44] I. G. McCarthy, R. G. Bower and M. L. Balogh, *Mon. Not. Roy. Astron. Soc.* **377**, 1457 (2007) [arXiv:astro-ph/0609314]; A. H. Gonzalez, D. Zaritsky and A. I. Zabludoff, arXiv:0705.1726 [astro-ph]; J. J. Mohr, B. Mathiesen and A. E. Evrard, *Astrophys. J.* **517**, 627 (1999) [arXiv:astro-ph/9901281].
- [45] D. J. Eisenstein *et al.*, *Astrophys. J.* **633**, 560 (2005) [arXiv:astro-ph/0501171].
- [46] J. Garcia-Bellido and T. Haugboelle, arXiv:0802.1523 [astro-ph].
- [47] W. J. Percival, S. Cole, D. J. Eisenstein, R. C. Nichol, J. A. Peacock, A. C. Pope and A. S. Szalay, *Mon. Not. Roy. Astron. Soc.* **381**, 1053 (2007) [arXiv:0705.3323 [astro-ph]].
- [48] F. Di Marco and A. Notari, *Phys. Rev. D* **73**, 063514 (2006) [arXiv:astro-ph/0511396]. T. Biswas and A. Notari, *Phys. Rev. D* **74**, 043508 (2006) [arXiv:hep-ph/0511207].
- [49] T. Biswas, R. Brandenberger, D. A. Easson and A. Mazumdar, *Phys. Rev. D* **71**, 083514 (2005) [arXiv:hep-th/0501194].
- [50] G. Ballesteros, J. A. Casas and J. R. Espinosa, *JCAP* **0603**, 001 (2006) [arXiv:hep-ph/0601134]; G. Ballesteros, J. A. Casas,

- J. R. Espinosa, R. Ruiz de Austri and R. Trotta, JCAP **0803**, 018 (2008) [arXiv:0711.3436 [hep-ph]].
- [51] D. H. Lyth and A. Riotto, Phys. Rept. **314**, 1 (1999) [arXiv:hep-ph/9807278].
- [52] D. J. H. Chung and A. Enea Romano, slow-roll Phys. Rev. D **73**, 103510 (2006) [arXiv:astro-ph/0508411]; J. E. Lidsey and R. Tavakol, of Phys. Lett. B **575**, 157 (2003) [arXiv:astro-ph/0304113]. J. M. Cline and L. Hoi, spectrum," JCAP **0606**, 007 (2006) [arXiv:astro-ph/0603403]. M. Joy, V. Sahni and A. A. Starobinsky, arXiv:0711.1585 [astro-ph].
- [53] R. Cen, Astrophys. J. **591**, L5 (2003) [arXiv:astro-ph/0303236]; B. Ciardi, A. Ferrara and S. D. M. White, Mon. Not. Roy. Astron. Soc. **344**, L7 (2003) [arXiv:astro-ph/0302451]; Z. Haiman and G. P. Holder, Astrophys. J. **595**, 1 (2003) [arXiv:astro-ph/0302403]; P. Madau, M. J. Rees, M. Volonteri, F. Haardt and S. P. Oh, Astrophys. J. **604**, 484 (2004) [arXiv:astro-ph/0310223]; S. P. Oh and Z. Haiman, Mon. Not. Roy. Astron. Soc. **346**, 456 (2003) [arXiv:astro-ph/0307135]; M. Ricotti and J. P. Ostriker, Mon. Not. Roy. Astron. Soc. **352**, 547 (2004) [arXiv:astro-ph/0311003] A. Sokasian, N. Yoshida, T. Abel, L. Hernquist and V. Springel, Mon. Not. Roy. Astron. Soc. **350**, 47 (2004) [arXiv:astro-ph/0307451]; R. S. Somerville and M. Livio, Astrophys. J. **593**, 611 (2003) [arXiv:astro-ph/0303017]; I. T. Iliev, G. Mellema, U. L. Pen, H. Merz, P. R. Shapiro and M. A. Alvarez, Mon. Not. Roy. Astron. Soc. **369**, 1625 (2006) [arXiv:astro-ph/0512187].
- [54] B. Fields and S. Sarkar, arXiv:astro-ph/0601514.
- [55] C. J. Copi, D. Huterer and G. D. Starkman, Phys. Rev. D **70** (2004) 043515 [arXiv:astro-ph/0310511]; C. J. Copi, D. Huterer, D. J. Schwarz and G. D. Starkman, Mon. Not. Roy. Astron. Soc. **367** (2006) 79 [arXiv:astro-ph/0508047]; P. Bielewicz, H. K. Eriksen, A. J. Banday, K. M. Gorski and P. B. Lilje, Astrophys. J. **635** (2005) 750 [arXiv:astro-ph/0507186]; D. Huterer, New Astron. Rev. **50** (2006) 868 [arXiv:astro-ph/0608318]. K. Land and J. Magueijo, Mon. Not. Roy. Astron. Soc. **378** (2007) 153 [arXiv:astro-ph/0611518].
- [56] J. Goodman, Phys. Rev. D **52**, 1821 (1995) [arXiv:astro-ph/9506068].
- [57] R. R. Caldwell and A. Stebbins, arXiv:0711.3459 [astro-ph].
- [58] C. Pahud, A. R. Liddle, P. Mukherjee and D. Parkinson, arXiv:astro-ph/0701481.
- [59] J. P. Zibin, Phys. Rev. D **78**, 043504 (2008) [arXiv:0804.1787 [astro-ph]].